# INFORMATION TO USERS

This manuscript has been reproduced from the microfilm master. UMI films the text directly from the original or copy submitted. Thus, some thesis and dissertation copies are in typewriter face, while others may be from any type of computer printer.

**The quality of this reproduction is dependent upon the quality of the copy submitted.** Broken or indistinct print, colored or poor quality illustrations and photographs, print bleedthrough, substandard margins, and improper alignment can adversely affect reproduction.

In the unlikely event that the author did not send UMI a complete manuscript and there are missing pages, these will be noted. Also, if unauthorized copyright material had to be removed, a note will indicate the deletion.

Oversize materials (e.g., maps, drawings, charts) are reproduced by sectioning the original, beginning at the upper left-hand corner and continuing from left to right in equal sections with small overlaps.

ProQuest Information and Learning
300 North Zeeb Road, Ann Arbor, MI 48106-1346 USA
800-521-0600

# A GENETIC APPROACH TO THE ROLE OF THE UBIQUITIN/PROTEASOME PATHWAY IN NEURODEGENERATION

*by*

ZONGMIN LI

A dissertation submitted to the Graduate Faculty in Biology in partial fulfillment of the requirements for the degree of Doctor of Philosophy, The City University of New York

2003

This manuscript has been read and accepted for the Graduate Faculty in Biology in satisfaction of the dissertation requirement for the degree of Doctor of Philosophy.

4/16/03
Date

Maria Figueiredo-Pereira
Chair of Examining Committee
Maria Figueiredo-Pereira, Hunter College

4/22/03
Date

Richard L. Chappell
Executive Officer
Dr. Richard L. Chappell

Thomas Schmidt-Glenewinkel
Dr. Thomas Schmidt-Glenewinkel, Hunter College

Patricia Rockwell
Dr. Patricia Rockwell, Hunter College

Peter Werner
Dr. Peter Werner, Albert Einstein College of Medicine

B. J. Wagner
Dr. B. J. Wagner,
University of Medicine and Dentistry of New Jersey

Supervising Committee

The City University of New York

# Abstract

## A GENETIC APPROACH TO THE ROLE OF THE UBIQUITIN/PROTEASOME PATHWAY IN NEURODEGENERATION

*by*

**Zongmin Li**

**Adviser: Dr. Maria E. Figueiredo-Pereira**

Involvement of the ubiquitin/proteasome pathway in neurodegeneration has gained support from a variety of studies. Although selective sets of neurons are affected in different neurodegenerative disorders, they share a common pathological feature: the occurrence of intracellular inclusions containing ubiquitinated proteins. Under homeostatic conditions, ubiquitinated proteins do not accumulate in cells since they undergo selective proteolysis by the ubiquitin/proteasome pathway. The inability to eliminate ubiquitinated proteins may result from a malfunction or overload of the ubiquitin/proteasome pathway or from structural changes in the protein substrates halting their degradation.

Our studies investigate the possibility that proteasome dysfunction is an important contributor to neurodegeneration. We previously established a mouse neuronal cell model in which proteasome inhibitors induced the formation of intracellular inclusions containing ubiquitinated proteins and lead to cell death. In the present study, disruption of proteasome activity was achieved by mutating the active site of its MC13 catalytic subunit. MC13, the β5 subunit of the mouse 20S proteasome, is responsible for the chymotrypsin-like activity that carries out the rate-limiting step in protein degradation through this pathway. The N-terminal Thr1 of MC13 is essential for its activity and was mutated to Ala1. MC13 and its mutant were tagged with a c-myc epitope. The fusion proteins were subsequently expressed in mouse neuronal HT4 cells and stable transfectants were selected with hygromycin B. Under homeostatic conditions, expression of the MC13 mutant (T1A) in HT4 cells impaired proteasome chymotrypsin-like activity without being dominant lethal. However, expression of the MC13 mutant hypersensitized the cells to oxidative stress resulting in the accumulation of ubiquitinated proteins in aggregates and leading to cell death. These findings clearly establish that selective

proteasome dysfunction causes neuronal changes that are common to a broad range of human neurodegenerative disorders. The genetic manipulation of proteasome activity in the neuronal cells provided the basis for establishing a transgenic mouse model to study the long-term effect of moderate proteasome dysfunction. Future studies with the cellular and the transgenic mouse models will provide important insights into the role of proteasome dysfunction in neurodegeneration.

# Acknowledgements

At this time, I would like to express my great gratitude to all who helped and supported me during this work. Especially, to my mentor and friend, Dr. Maria Figueiredo-Pereira, for all the kind support, encouragement and intellectual guidance. When I made progress or ran into difficulties during my study, she is always the first person for me to share the happiness with or ask for help. Working in her lab is a wonderful experience and what I have learned from her will continually guide my future scientific career.

To Dr. Patricia Rockwell, for all her kindness in technical support and training me with advanced molecular biotechniques. Her suggestions helped me solved some of the major technical difficulties in this study. To all my other thesis committee members, Drs. Thomas Schmidt-Glenewinkel, Peter Werner and BJ Wagner, for their time and advice when requested. Especially to Dr. Peter Werner, who provided me the kind support in Albert Einstein College of Medicine to carryout the work on transgenic mice. I would also like to thank Dr. Benjamin Ortiz for his invaluable advice on generating the transgenic mice. Dr. Willy Maledo from Dr.

Filbin's lab also provided technical support on the β-glactosidase *in-situ* staining of HT4 cells transfected with *LacZ*.

I would like to thank Mrs. Hongmei Yuan, a former lab technician, who trained me so patiently during my beginning times in science. Dr. Elaine Wang, a former postdoc and Buyi Zhang, a rotational student, did part of the work on the site-directed mutagenesis on MC13 cDNA. A lot of thanks to all other members in our laboratory who supported and helped me during these years.

Special thanks to my parents and sisters in China, and my lovely wife for their understanding and endless support. Without their love, I would have not been able to come through all the difficulties and grow as a scientist.

Finally, I would like to dedicate this thesis to my baby to be born in August 2003.

# Table of Contents

# List of Figures and Tables

# Table of Abbreviations

| | |
|---|---|
| AD | Alzheimer's disease |
| BCA | bicinchoninic acid |
| BGH | bovine growth hormone |
| CMV | cytomegalovirus |
| CNS | central nervous system |
| HNE | 4-hydroxy-2-nonenal |
| IPTG | isopropylthio-β-D-glactoside |
| LB | Luria-Bertani |
| MPTP | 1-methyl-4-phenyl-1, 2, 3, 6-tetrahydropyridine |
| MTT | 3-(4,5-dimethylthia-zol-2-yl)-2,5-diphenyl tetrazolium Bromide |
| NEB | New England Biolabs |
| NFT | neurofibillary tangles |
| NGF | nerve growth factor |
| PCR | polymerase chain reaction |
| PD | Parkinson's disease |
| ROS | reactive oxygen species |
| SOD | superoxide dismutase |
| Ub | ubiquitin |
| UBP | ubiquitin-specific processing proteases |
| UCH | ubiquitin carboxyl-terminal hydrolases |

# *Chapter I*

# Introduction

Before the 1980s, protein degradation was considered to be a non-specific, dead-end process and very few studies were carried out in this field. The discovery of lysosomes by Christian de Duve in 1955 did not significantly change this situation, because protein degradation through these organelles is not substrate-specific and is mostly involved in the degradation of membrane-bound or extracellular proteins that are internalized by endocytosis (Glickman and Ciechanover, 2002). In the early 1980s, the discovery of the multicatalytic proteasome complex revolutionized the field and since then tremendous progress has been made in our understanding of proteasome structure and function (Ding and Keller, 2001). It is now clear that degradation of cellular proteins by proteasomes is a highly complex, temporally controlled and tightly regulated process that plays major roles in a variety of basic pathways during cell life and death as well as in health and disease (Glickman and Ciechanover, 2002). With the multitude of substrates identified and the myriad processes involving protein degradation through the ubiquitin/proteasome pathway, it is not surprising that aberrations in this pathway are implicated in the pathogenesis of many diseases, such as cancer and neurodegeneration (Glickman

and Ciechanover, 2002). In this study, we used a genetic approach to investigate the role played by the ubiquitin/proteasome pathway in neurodegeneration.

## 1. Protein Degradation through the Ubiquitin/Proteasome Pathway.

The ubiquitin/proteasome pathway is the major pathway for regulated non-lysosomal degradation of intracellular proteins in eukaryotes. Short-lived proteins such as cell cycle regulators and transcription factors, as well as abnormal proteins from the cytosol, nucleus and endoplasmic reticulum are specifically recognized and degraded through this pathway (Coux et al., 1996; Chen and Hochstrasser, 1996). The ubiquitin/proteasome pathway is of vital importance for maintaining homeostasis and normal function of eukaryotic cells (Heinemeyer et al., 1991).

Two major steps are involved in protein degradation through the ubiquitin/proteasome pathway: ubiquitination and degradation. Ubiquitin (Ub) is a small protein of 76 amino acids and is crucial to the degradation of many

cytosolic, nuclear and endoplasmic reticulum proteins (Hochstrasser, 1995). It is so called ubiquitin because it

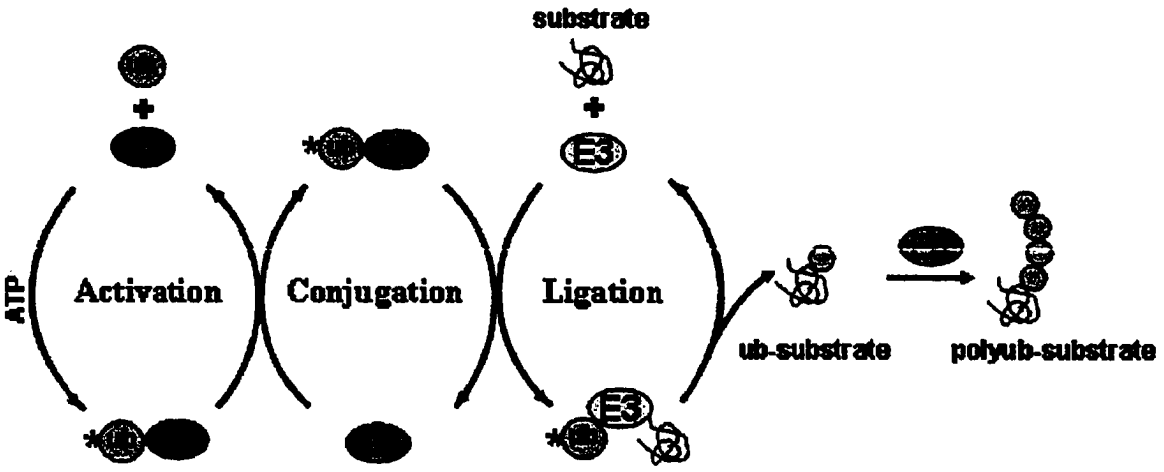


**Figure 1.1 - Protein ubiquitination.** First, a high energy thioester bond is formed between ubiquitin (Ub) and a ubiquitin-activating enzyme (E1). This reaction requires ATP hydrolysis. Secondly, the activated ubiquitin is transferred to a ubiquitin conjugating enzyme (E2). Thirdly, the activated ubiquitin (*) is ligated, via an isopeptide bond, to the protein substrate by a ubiquitin ligase (E3). Lastly, the ubiquitin chain is elongated by an ubiquitin-chain elongating factor (E4) which drives polyubiquitin chain (poly Ub) assembly.

is ubiquitous to every eukaryotic cell. There are, at least, three human ubiquitin genes, two of which, the *polyubiquitin B* and *C* genes, contain heat-shock promoters (Mayer et al., 1991). Ubiquitination of proteins is a complex ATP-dependent process (Figure 1.1) in which ubiquitin is sequentially activated by ubiquitin-activating enzymes (E1), transferred to ubiquitin-conjugating enzymes

(E2) and then ligated to protein substrates by ubiquitin ligases (E3) (Scherrer and Bey, 1994). Ubiquitin is linked to the substrate through formation of an isopeptide bond between the C-terminus of ubiquitin (glycine-76) and the side chain of a lysine residue of the substrate (Scherrer and Bey, 1994). Finally, additional ubiquitin molecules are attached to the monoubiquitinated substrate by a ubiquitin-chain elongating factor (E4), which facilitates the formation of polyubiquitin chains (Figure 1.1) (Koegl et al., 1999). At least four molecules of ubiquitin, forming a tetraubiquitin chain, need to be attached to the substrate to ensure efficient recognition and degradation by the 26S proteasome machinery (Cook et al., 1994). Longer polyubiquitin chains exhibit increased binding affinity for the 26S proteasome, thus enhancing the degradation of the polyubiquitinated substrate (Pickart, 1997).

Ubiquitin is removed from ubiquitinated proteins by de-ubiquitinating enzymes, which also disassemble polyubiquitin chains. More than 90 genes encoding de-ubiquitinating enzymes have been identified, making them the largest family of enzymes involved in the ubiquitin pathway (Chung and Baek, 1999). There are two major classes of de-ubiquitinating enzymes: (1) Ubiquitin carboxyl-

terminal hydrolases (UCHs) that remove small amides, esters, peptides and small proteins at the carboxyl terminus of ubiquitin, and (2) ubiquitin-specific processing proteases (UBPs) which disassemble the polyubiquitin chains and may edit the ubiquitination state of proteins (Wilkinson, 1997).

Covalent binding of ubiquitin to proteins marks them for subsequent degradation by the ubiquitin/ATP dependent proteinase known as the 26S proteasome, which is a multicomponent enzymatic complex with a native molecular weight of approximately 2000kDa (Coux et al., 1996). The 26S proteasome complex is composed of two major components (Figure 1.2). A cylinder-like structure, known as the 20S proteasome, is located in the center and is the catalytic core of the enzyme. A regulatory component, known as the 19S particle, which may be attached to each end of the cylinder-like 20S proteasome (DeMartino and Slaughter, 1999a). The 19S particle is a muticomponent complex itself. It is composed of more than 20 proteins which are subdivided into three groups: a base which confers the complex its ATPase activity, a lid which can specifically bind to polyubiquitin-tagged substrates and a third group

which may have some deubiquitination activity (DeMartino and Slaughter, 1999b) (Figure 1.2).

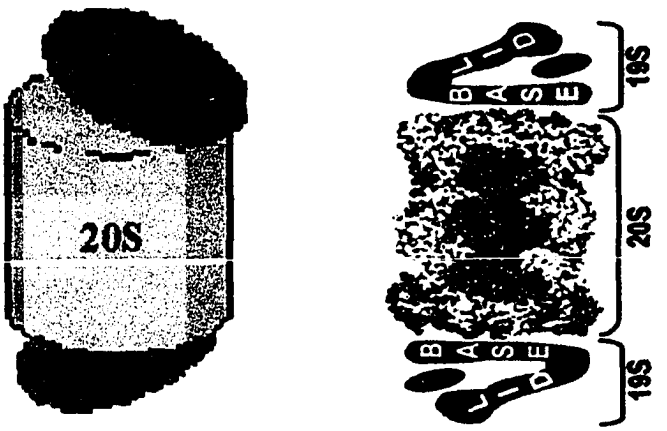


**Figure 1.2 - The structure of the 26S proteasome.** Its two major particles, the 20S particle (20S proteasome) which is the catalytic core, and the 19S particle (PA700) which is the regulatory component, require ATP hydrolysis to assemble into the 26S proteasome. The 19S lid confers ubiquitin/ATP-dependency to proteasome proteolysis. The 19S base has ATPase and chaperone-like activity. The diagram on the left is the schematic representation of the two major particles in the complex. The midlongitudinal view of the 20S proteasome in the diagram on the right was drawn from 1ryp.pdb (Groll et al. 1997 ).

The eukaryotic 20S proteasome is composed of 28 subunits, which are subdivided into two major categories, α and β, according to their homology to the two types of proteasome subunits in Archeabacteria, *T. acidophilium* (Groll et al., 1997). The 28 subunits of the 20S proteasome are arranged as a stack of four rings with seven different subunits in each ring (Figure 1.3). The two outer rings are identical and contain α subunits only. The two inner rings

are also identical and they are composed of β subunits only. This special subunit arrangement is a novel topology characterized by an αββα sandwich (Figure 1.3), revealing the fact that the eukaryotic 20S proteasome is a dimmer. Each half of the 20S proteasome is composed of 14 different

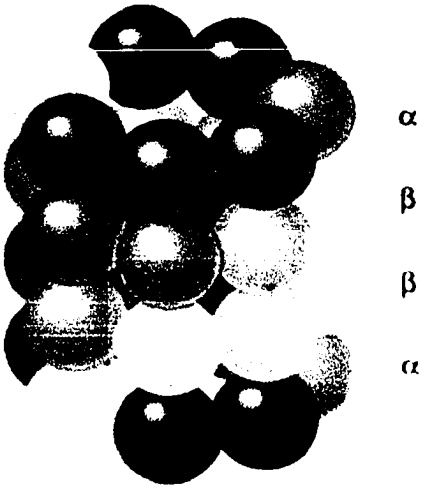


**Figure 1.3 – The structure of the 20S proteasome (Affinity, UK).** Each colored sphere represents one subunit of the 20S proteasome. The 28 subunits are arranged in a novel topology characterized by an αββα sandwich.

subunits, seven of which are α-type and seven are β-type (Groll et al., 1997). These 14 different subunits are encoded by 14 different genes in eukaryotes. Assembly of this particle from precursor subunits is a complex process that requires the assistance of a short-lived chaperone (Ramos et al., 1998).

The α-type subunits, comprising the two outer rings of the 20S proteasome, provide binding sites for regulatory particles and form a gated channel leading to the inner catalytic chamber. The β-type subunits contain the active sites of the 20S proteasome. Among the 14 different subunits of the 20S proteasome, only three of the β subunits are found to contain the active sites for protein degradation. The functions of the remaining four β subunits are still under investigation (Groll et al., 1997; Dick et al., 1998). Proteasomes are placed in the family of Ntn (N-terminal nucleophile) hydrolases because of their catalytic mechanism, which includes an N-terminal nucleophilic threonine in the active site of the catalytically involved β subunits (Brannigan et al., 1995).

The three β subunits containing active sites are first synthesized as precursor proteins known as proproteins. Each of these precursors contains a propeptide at the N-terminus. In order to mature and become active, the N-terminal propeptide of each proprotein must be cleaved (Chen and Hochstrasser, 1996). This cleavage exposes the N-terminal residue Thr+1 of the mature β subunits to the inner cavity of the catalytic core. This objective is achieved by

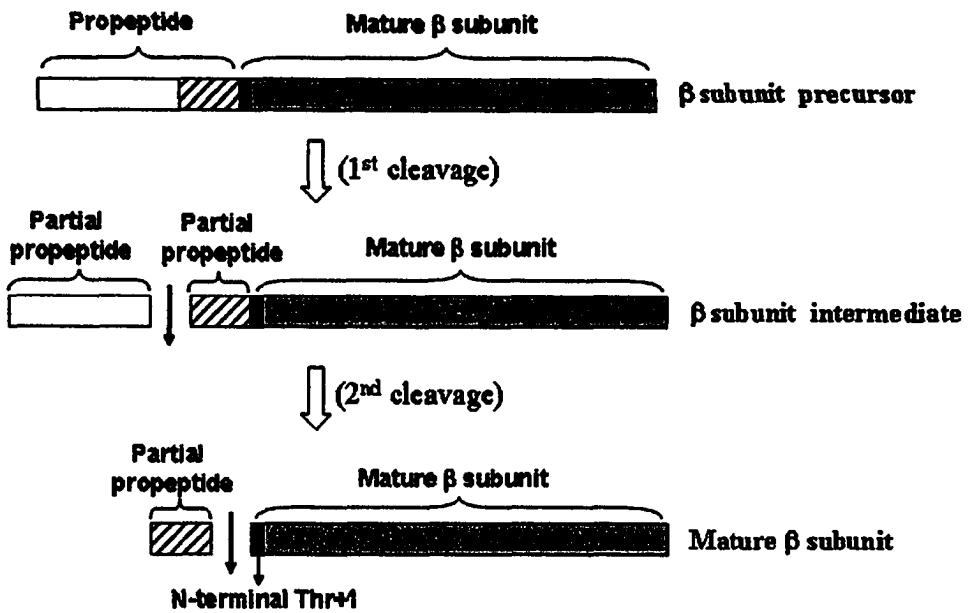


**Figure 1.4 - Two-step autocatalysis model of β subunit maturation in mammalian 20S proteasome.** In this model, the maturation of the β subunit is achieved by a two-step cleavage. The first cleavage occurs within the propeptide, resulting in a short-lived intermediate that contains a short N-terminal extension. Shortly thereafter, the second cleavage follows, resulting in the full removal of the propeptide and final maturation of the β subunit with the N-terminal Threonine exposed as the active site.

a process known as autocatalytic processing, which occurs right after the full assembly of the 20S proteasome cylinder (Schmidt and Kloetzel, 1997). Studies with yeast have shown that the N-terminal propeptide is required for the incorporation of β subunits into the proteasome complex. Remarkably, the propeptide functions in *trans*, suggesting that it serves a chaperon-like function in proteasome

biogenesis (Chen and Hochstrasser, 1996). Studies in mammals demonstrated that maturation of β subunits is a two-step autocatalysis in which an intact Gly-1/Thr+1 consensus motif coupled to Lys33 is essential for correct processing. During the autocatalytic processing, Thr+1 acts as the nucleophile and Lys33 as the proton donor/acceptor (Schmidtke et al., 1996). The first cleavage occurs within the propeptide, resulting in a short-lived intermediate that represents the semi-matured β subunits with a short N-terminal extension. Shortly thereafter, the second cleavage follows, resulting in the full removal of the propeptide and final maturation of the β subunits (Figure 1.4) (Schmidtke et al., 1996). Based on this autocatalytic processing model of β subunits, it is quite obvious that the N-terminal Thr+1 is crucial for both the autocatalytic processing and the proteolytic activity of the 20S proteasome. Studies in yeast indicated that mutations of the Thr+1 of β subunits did not interfere with their incorporation into the quaternary structure of the 20S proteasome (Chen and Hochstrasser, 1996). However, the mutation impaired the autocatalytic processing of β subunits. Most of the mature β subunit mutants were detected

as intermediate products of the first cleavage (Chen and Hochstrasser, 1996).

| | Yeast | Mouse | Human | Activity |
|---|---|---|---|---|
| β1 | Pre3 | mC5 | hC5 | caspase-like |
| β2 | Pup1 | mC10II | hC10II | trypsin-like |
| β5 | Pre2 | **MC13** | MB1 | chymotrypsin-like |

**Table 1.1 - Three β subunits bearing the active sites of the 20S proteasome and their homologues in yeast, mouse and human.** The peptidase activity conferred by each of the three subunits is listed in the right most column. The β5 subunit of the mouse 20S proteasome, which is the subject of this study, is shown in bold.

The three β subunits bearing the active sites of the 20S proteasome are β1, β2 and β5. They are responsible for the caspase-like, trypsin-like, and chymotrypsin-like activities of the 20S proteasome, respectively. They were first identified in yeast as Pre3, Pup1 and Pre2, respectively (Groll et al., 1999). Their homologues in mouse and human are listed in Table 1. The chymotrypsin-like activity associated with the β5 subunit is responsible for the first and rate-limiting step in protein degradation through this pathway (Kisselev et al., 1999). During this

first step, protein substrates are cleaved into large peptide fragments. In the second step of degradation, the caspase-like activity associated with the β1 subunit and the trypsin-like activity associated with the β2 subunit will further break down the fragments generated in step one. These two steps of protein degradation suggest a "bite-chew" processive model for protein breakdown through the ubiquitin-proteasome pathway. An alternative non-processive model of degradation was proposed in recent studies with higher organisms. The non-processive mechanism comprises multiple, independent cleavages with dissociation of degradation intermediates. These studies proposed a more general model for protein degradation by the proteasome (Wang et al., 1999).

However, in any of the models currently proposed, the chymotrypsin-like activity conferred by the β5 subunit is essential for protein degradation by proteasomes. Studies with yeast (Heinemeyer et al., 1993) and *Drosophila* (Belote and Fortier, 2002) demonstrated that a functional β5 subunit is essential for survival. Based on these findings, in the current study we ensured that not all of the 20S proteasome chymotrypsin-like activity was eliminated. Accordingly, the

β5 mutant was overexpressed in mouse neuronal HT4 cells with an endogenous β5 wild type gene.

## 2. Aging, Oxidative Stress, and Proteasome Dysfunction.

Aging is a complex process that is accompanied by the decline of different physiological functions of an organism along its life (Carrard et al., 2002). During this progressive and irreversible process, many diseases may develop in different organ systems of the organism; among them are the age-dependent devastating neurodegenerative disorders, such as Alzheimer's disease (AD) and Parkinson's disease (PD). Understanding the relationship between aging and proteasome dysfunction may provide additional insights into the pathological mechanisms underlying neurodegeneration.

One important feature of the aging process is the accumulation of proteins damaged or modified by oxidative stress (Van Remmen et al., 1996). Production of reactive oxygen species (ROS) is known to increase with age and in

certain age-related diseases such as PD (Jenner, 2001). Antioxidants, such as glutathione, α-tocopherol (vitamin E), carotenoids and ascorbic acid will react with most of ROS and prevent their damaging effects. In addition, antioxidant enzymes, such as catalase and glutathione peroxidase, detoxify $H_2O_2$ by converting it to $O_2$ and $H_2O$. However, when ROS levels exceed the antioxidant capacity of a cell, a deleterious condition known as oxidative stress occurs (Klein and Ackerman, 2003).

ROS are molecules formed during aerobic respiration by the mitochondrial electron transport chain, in which ATP is produced and oxygen molecules are reduced to a radical intermediate with a single unpaired electron. The radical intermediate can exist as a superoxide anion, $^{\bullet}O_2^-$. The superoxide anion $^{\bullet}O_2^-$ can subsequently be converted by superoxide dismutase (SOD) to hydrogen peroxide $H_2O_2$ that can generate the hydroxyl radical $^{\bullet}OH$ through the Fenton reaction (Nakagawara et al., 1981). Damages to macromolecules occurring upon aging are mainly the result of reactions implicating these ROS, which are also referred to as free radicals (Beckman and Ames, 1998). Nucleic acids, lipids and proteins are all targets for ROS attack.

Almost all amino acids within proteins can be oxidized by ROS, sulfur-containing (cysteine and methionine) and aromatic (tyrosine and tryptophan) amino acids being the most susceptible (Berlett and Stadtman, 1997;Davies, 1987). Very few repair systems for oxidatively damaged proteins are currently identified. ROS modification can also promote partial unfolding of cellular proteins, resulting in exposure of previously buried hydrophobic domains to proteolytic enzymes (Grune et al., 1997; Chao et al., 1997) and to ubiquitin-conjugating enzymes (Sadis et al., 1995). Therefore, one other important cellular antioxidant mechanism is an increase in intracellular proteolysis by proteasomes (Shringarpure et al., 2003; Figueiredo-Pereira ME and Rockwell, 2001).

In some studies, degradation of oxidized proteins by the 20S proteasome was shown to be independent of ubiquitination (Grune et al., 1997). However, other studies with bovine lens epithelial cells indicate that removal of oxidatively modified proteins can be achieved by the ubiquitin-proteasome pathway (Shang and Taylor, 1995; Shang et al., 2001). In addition, *in vivo* studies with mice exposed to oxidative stress by intraperitoneal injections of ferric nitrilotriacetate, demonstrated that kidney

proteins modified by the lipid peroxidation product 4-hydroxy-2-nonenal (HNE) undergo ubiquitination (Okada et al., 1999). These findings suggest that oxidatively modified proteins, which may accumulate with age and under certain pathological conditions, are eliminated by the proteasomal machinery.

Ubiquitin-protein conjugates are found to accumulate with age in different tissues. The age-related accumulation of oxidized and ubiquitinated proteins and the slowing down of protein turnover raise the possibility that proteasome activity is impaired with aging. Mechanisms underlying age-related proteasome dysfunction have been addressed by many investigators. Recent studies using microarray technology showed that transcription of several genes encoding either 20S or 26S proteasome subunits declines with age (Ly et al., 2000; Lee et al., 1999). Furthermore, components of the ubiquitin/proteasome pathway can also be modified by oxidative stress leading to impairment of this pathway (Bulteau et al., 2000). Aging may also influence the proteasome activities due to the formation of inhibitory damaged proteins associated with oxidative stress (Friguet and Szweda, 1997; Conconi and Friguet, 1997). The combination of these effects may contribute to the age-

related decline of proteasome activity. However, the role played by loss of proteasome function in neurodegeneration is not fully characterized.

### 3. Oxidative Stress and Neurodegeneration.

Increasing evidence supports the involvement of oxidative stress in neurodegeneration. For example, transgenic mice lacking the α-tocopherol transfer protein develop spinal cord and retinal degeneration, leading to gait abnormalities at 1 year of age (Yokota et al., 2001). These behavioral and pathological changes were largely prevented with α-tocopherol supplementation. In addition, *SOD2*$^{-/-}$ transgenic mice develop brainstem and cortical vacuolization at 12 days of age, also leading to gait abnormalities (Melov et al., 1998). These results indicate that the loss of antioxidant genes can lead to neuronal loss.

Studies with autopsied brains of AD patients showed a co-localization of neurofibrillary tangles and senile plaques with high levels of oxidative stress markers, such as DNA oxidation, protein oxidation and lipid peroxidation (Markesbery and Carney, 1999). In addition, increased levels of catalase, glutathione peroxidase and glutathione reductase were detected, by RT-PCR analysis, in the hippocampus and inferior parietal lobe of brains of AD patients (Aksenov et al., 1998). Signs of oxidative stress, such as lipid peroxidation and a decline in reduced glutathione, were also detected in the substantia nigra of PD brains (Fahn and Cohen, 1992). Extensive post-mortem tissue studies detected a co-localization of oxidative/nitrative products with the intracellular inclusions characteristic of AD and PD brains (Giasson et al., 2002). Oxidative damage is also reported in several other age-related neurodegenerative diseases, including Huntington's disease, progressive supranuclear palsy, amyotrophic lateral sclerosis and prion disorders, all of which have abnormal protein aggregation as a major component of their pathology (Albers and Augood, 2001; Butterfield and Kanski, 2001;Kim et al., 2001). Whether oxidative stress is involved in the development and/or progression of these disorders, or if it is merely associated with the end-

stage of these diseases, is currently not clear (Klein and Ackerman, 2003).

As discussed previously, oxidative stress can be induced by aerobic respiration in mitochondria. In the Central Nervous System (CNS) other mechanisms can lead to oxidative stress, such as oxidative metabolism of dopamine and exposure to environmental chemicals such as 1-methyl-4-phenyl-1, 2, 3, 6-tetrahydropyridine (MPTP), rotenone and paraquat (Chun et al., 2001). To address the relationship between oxidative stress and the ubiquitin/proteasome pathway in neurodegeneration, we chose to treat mouse neuronal HT4 cells with the heavy metal cadmium ($Cd^{++}$). Although cadmium is redox inactive and cannot generate reactive oxygen species directly, the heavy metal is a well established oxidative stressor as it depletes glutathione and protein-bound sulfhydryl groups resulting in rises in the intracellular levels of ROS, such as superoxide ion, hydroxyl radicals and hydrogen peroxide (Stohs and Bagchi, 1995).

Cadmium is a heavy metal widely found in our environment. Humans are exposed to heavy metals from

numerous sources, including contaminated air, water, soil and food (Beyersmann and Hechtenberg, 1997). Besides its adverse effects on the kidneys and testes, cadmium was also shown to affect the nervous system and is associated with learning disabilities and over reactivity in children (Pihl and Parkes, 1977). Studies indicate that the uptake of cadmium into mammalian cells does not occur by passive diffusion but rather by an active transport mechanism, in which the voltage-gated calcium channel may play an important role (Klug et al., 1988; Hinkle and Osborne, 1994;Hechtenberg and Beyersmann, 1994). After being taken up into the cells, cadmium accumulates intracellularly by binding to cytoplasmic and nuclear proteins. Cadmium is removed from the human body at a slower pace than many other environmental contaminants. Its half-life is in the order of 20 years (Kjellstrom, 1971; Tsuchiya et al., 1976). When the accumulation of cadmium in cells reaches a cytotoxic level, it starts to inhibit the biosynthesis of DNA, RNA and proteins. It also induces lipid peroxidation, DNA strand breaks and chromosome aberrations (Beyersmann and Hechtenberg, 1997). Cadmium also enhances the expression of several classes of genes at concentrations of a few μM. The heavy metal stimulates expression of immediate early genes (*c-fos, c-jun and c-myc*), the tumor suppressor

gene *p53* and genes encoding for the synthesis of protective molecules including metallothioneins, glutathione as well as stress (heat shock) proteins (Beyersmann and Hechtenberg, 1997).

Although cadmium is not a Fenton metal and thus, by itself, is unable to generate ROS, it may enhance accumulation of free radicals by hindering the antioxidant defense system (Shukla and Chandra, 1987). Studies showed that this heavy metal may increase lipid peroxidation in organs such as the brain, which is particularly sensitive to cadmium toxicity (Acan and Tezcan, 1995). Earlier studies (Jungmann et al., 1993) suggested a close link between the ubiquitin/proteasome pathway and cadmium cytotoxicity because yeast mutants deficient in a specific ubiquitin-conjugating enzyme (UBC7) or a proteasome subunit (PRE1) were hypersensitive to the heavy metal. Moreover, our previous studies with neuronal cells (Figueiredo-Pereira et al., 1998; Figueiredo-Pereira and Cohen, 1999) demonstrated that cadmium disrupts intracellular sulfhydryl homeostasis, leading to the accumulation of ubiquitinated proteins and to a loss in cell viability. In the current study, we compared the vulnerability of stable transfected mouse neuronal HT4

cells expressing wild type or mutant MC13 subunits of the 20S proteasome to cadmium-induced oxidative stress.

**4. Proteasome Dysfunction and Neurodegeneration.**

In neurodegenerative disorders such as AD and PD, there is an irreversible loss of neuronal cells in particular regions of the brain, such as neocortex and hippocampus in AD and substantia nigra in PD. Although selective sets of neurons are affected in different neurodegenerative disorders, most of them share an intriguing pathological feature, namely the accumulation of intracelluar protein aggregates known as inclusion bodies. These diseases are, therefore, associated with an inability of the neuron to degrade these protein aggregates which may, over time, affect neuronal function and eventually lead to neurodegeneration (Schulz and Dichgans, 1999).

The accumulation of ubiquitin-protein conjugates in inclusions was first detected in neurofibrillary tangles (NFT) found in brains of AD patients (Mori and Ihara, 1987). Additional inclusions containing ubiquitinated proteins were subsequently identified in a whole host of

neurodegenerative diseases (Lowe et al., 1988), suggesting that the ubiquitin/proteasome pathway plays an important role in neurodegeneration.

In general, high levels of ubiquitinated proteins do not accumulate in healthy cells as they are rapidly degraded by the ubiquitin/proteasome pathway. The inability to eliminate these modified proteins may result from a functional failure of the ubiquitin/proteasome pathway or from structural changes in the protein substrates rendering them inaccessible to the degradation component (Figueiredo-Pereira ME and Rockwell, 2001). The mechanisms underlying the formation of these ubiquitinated protein aggregates and their relationship to neuronal cell death are still not clear.

Recent studies have provided additional support for a role of proteasome dysfunction in neurodegeration. Keller and colleagues compared proteasome activities in brain specimens from AD and age- and sex-matched controls. The chymotrypsin-like and caspase-like activities of the 20S proteasome were found to be significantly lower in the hippocampus and parahippocampal gyrus, superior and middle temporal gyri and inferior parietal lobule of AD brains

than in controls (Keller et al., 2000a). A similar decline in proteasome activity was identified in the substantia nigra of PD brains (McNaught and Jenner, 2001) and after ischemia-reperfusion injury (Keller et al., 2000b). Whether the decline in proteasome activity associated with neurodegeneration is the causative factor of these pathological conditions or is just a secondary effect of neurodegeneration is not well established.

To elucidate the cellular events associated with proteasome dysfunction in neurodegeneration, we previously treated neuronal cells with proteasome inhibitors, such as epoxomycin and PSI [N-benzyloxycarbonyl-Ile-Glu(O-*tert*-butyl)-Ala-leucinal] (Rockwell et al., 2000). However, most of the neurodegenerative disorders are age-dependent, long-term progressive diseases and proteasome inhibitors are toxic, unstable, unsuitable for long-term studies and, in many instances, unspecific. To overcome these difficulties, in the present study we used a genetic approach to specifically impair the chymotrypsin-like activity of the 20S proteasome. The active site of the β5 subunit of the mouse 20S proteasome was mutated by site-directed mutagenesis. The mutated subunit was subsequently expressed in the mouse neuronal HT4 cell line. Cellular responses to

impairment of proteasome activity by this genetic manipulation were further investigated under conditions of oxidative stress. These studies are the first to demonstrate that a proteasome mutation that reduces its activity triggers cellular responses that are common to a broad range of human neurodegenerative disorders.

# *Chapter II*

# Materials and Methods

***Site-directed Mutagenesis*** - Mutagenesis was conducted in three steps with the QuickChange™ Site-Directed Mutagenesis Kit (Stratgene, CA). **Step 1:** To a 500µl eppendorf tube, we added 5µl of 10X reaction buffer (provided in the kit), 1µl of dNTP mix (contains 2.5mM of dNTP, provided in the kit), 1µl of *Pfu* DNA polymerase (2.5U/µl, provided in the kit), 50ng of MC13 β5 cDNA (MC13, a gift from Dr. P. Kloetzel, Berlin, Germany), 41µl of $dH_2O$ and 1µl of primer #1 (0.1µM). The sequence of primer #1 was: 5'-GCCCACGGC***g***C***c***ACCACACTCGCCTTC-3' according to the MC13 cDNA sequence (Frentzel et al., 1992). The lower case ***g*** and ***c*** represent the two nucleotides within the N-terminal threonine codon of the MC13 subunit that were mutated. A second 500µl eppendorf tube contained all of the same components listed above, except that 1µl of primer #2 (0.1µM) was added instead of primer #1. The sequence of primer #2 was: 5'-GAAGGCGAGTGTGGT***g***G***c***GCCGTGGGCC-3', which is the reverse (antisense) and complement strand of primer #1. The lower case ***g*** and ***c*** also represent the nucleotides within the N-terminal threonine codon of the MC13 subunit that were mutated. After vortexing, the Polymerase Chain Reactions (PCR) in each tube was set-up as follows: 95°C for

30sec then 8 cycles of: 95°C for 30sec, 55°C for 1min and 68°C for 11min. The final temperature was set at 4°C for storage. **Step 2:** 25µl of the reaction mixture from each step 1 tube were added into a new PCR tube and mixed well. The new PCR was set-up as follows: 95°C for 30sec then 18 cycles of: 95°C for 30sec, 55°C for 1min and 68°C for 11min. The final temperature was set at 4°C for storage. **Step 3:** 1µl of the *DpnI* restriction enzyme (10U/µl, provided in the kit) was added to the PCR reaction from step 2 followed by incubation at 37°C for 1hr. After the *DpnI* digestion, 3µl of the final mixture was used in the transformation described below. The successfully mutated MC13 was designated as Muta-1.

***Transformation*** - 50µl of Epicurian Coli® XL1-Blue supercompetent cells (Strata-gene, CA) were aliquoted into prechilled 15ml Falcon 2059 polypropylene tubes. 0.8µl of β-mercaptoethanol was added to each tube, to a final concentration of 25mM. Contents in the tubes were mixed by swirling gently, followed by incubation on ice for 10 minutes. 3µl of the PCR reaction mixture or 50ng of DNA templates were added to the 50µl of bacterial cells and swirled gently, followed by incubation on ice for 30

minutes. After the incubation, tubes were heat-pulsed in a 42°C water bath for 45 seconds, immediately followed by incubation on ice for 2 minutes. We then added 0.9ml of preheated (42°C) Luria-Bertani (LB) Medium to each tube and incubated the tubes at 37°C for 1 hour in an Incubator Shaker (New Brunswick Scientific, Edison, NJ) at 225-250rpm. Finally, less than 200µl of the transformation mixture were spread onto LB plates containing 100ug/ml ampicillin, followed by overnight incubation at 37°C. In order to conduct the white-blue screening, 40µl of a stock solution of X-gal (50mg/ml in dimethylformamide, Promega, WI) and 4µl of a solution of isopropylthio-β-D-glactoside (IPTG) (200mg/ml, Promega, WI) were spread evenly on the pre-heated plates (37°C). These plates were then incubated at 37°C for at least 30 minutes before the cells were plated.

***Restriction Analysis*** – The restriction enzymes *BamHI*, *KpnI*, *SfoI*, *MfeI* and *NaeI* used in this study were purchased from New England Biolabs (NEB), MA. Restriction analysis reactions were carried-out in a 37°C water bath for 2 hours except for the double digestion with *BamHI and Kpn* or *BamHI* and *SfoI*. Each of these two reactions was carried-out in a

two-step sequential digestion. In the first step, the DNA templates were digested in a 37°C water bath for 2 hours with either *Kpn* or *SfoI* which are compatible with low-salt NEB buffers. In the second step, *BamHI* and the high salt NEB buffer for *BamHI* were added to the reaction mixture followed by incubation at 37°C for two additional hours. The final products of each reaction were subjected to electrophoresis on 1% or 2% agarose gels containing 0.67μg/ml Ethidium Bromide (Promega, WI), according to the size of the fragments generated.

***Subcloning of MC13 and Muta-1 into a mammalian expression vector*** - To be able to express the two genes in mammalian cells, the MC13 and the Muta-1 cDNAs were subcloned into the pcDNA3.1/hygro(-) mammalian expression vector (Invitrogen, CA).

***DNA Sequencing*** - pBluescriptSK(+) and pcDNA3.1/hygro (-) vectors containing MC13(c-myc) or Muta-1(c-myc) cDNA were sequenced by the DNA Sequencing Facility at the Biotechnology Center, Utah State University following the standard Automated DNA Sequencing Protocol.

***Cell Cultures*** - HT4 cells are a mouse neuroblastoma cell line immortalized with a recombinant temperature sensitive mutant of the SV40 large T antigen (Whittemore et al., 1991). Stocks were maintained at the permissive 33°C temperature. When transferred to 39°C (non-permissive temperature), their growth rate is significantly decreased and they differentiate with neuronal morphology, express neuronal antigens, synthesize and secrete nerve growth factor (NGF) and express receptors for NGF (Whittemore et al., 1991). Stocks of HT4 cells were maintained at 33°C in Dulbecco's modified Eagle's medium containing 5% normal fetal bovine serum, and 100 units/ml penicillin, 100 µg/ml streptomycin in 5% $CO_2$. Stable transfectants were maintained in 0.6mg of hygromycin B (Invitrogen, CA) per ml of media. To induce differentiation, cells were transferred to 39°C, where they were kept for 3 days. Following the period of differentiation, cells were maintained for 24hr at 37°C in the absence of hygromycin B prior to the experimental treatments.

***Transfection*** - HT4 cells were plated 24 hours before transfection on 100mm dishes at the density of 1.0 X $10^5$ cells per ml of media. The Effectene® reagent kit (Qiagen, CA) was used in this study. 4µg of DNA were first diluted

into 300µl of buffer QC (provided in the kit). 32µl of Enhancer (provided in the kit) were then added followed by incubation for 5 minutes at room temperature. 40µl of Effectene reagent were added next and the mixture was incubated for 10-15 minutes at room temperature to allow the formation of DNA-Reagent complexes. Finally, 3ml of serum-containing media were added to dilute the DNA-Reagent complex and the whole mixture was applied to the cells, which were pre-washed two times with PBS. 7ml of fresh media were lastly added to the cells. After incubation at 37°C with 5% $CO_2$ for 16, 24 or 48 hrs, the cells were harvested in hot 1% SDS buffer in 0.01M Tris-EDTA, pH=7.5.

For stable transfection, after incubation at 37°C with 5% $CO_2$ for 48 hrs, the cells were split into new 100mm dishes with very low density to allow formation of single colonies. 1000µg/ml hygromycin B was used to select the stable colonies.

***Protein Concentration Assay*** - The Bicinchoninic Acid (BCA) Reagent Kit (Pierce, IL) was applied in this study to analyze the protein concentration of HT4 cell lysates. The assay was set-up in a 96-well plate. To establish a

standard curve, 25µl of SDS buffer (1% SDS, 0.01M Tris-EDTA, pH=7.5) or 25µl of each of standard solutions containing 0.1mg/ml, 0.2mg/ml, 0.4mg/ml, 0.8mg/ml and 2.0mg/ml of Bovine Serum Albumin in the same SDS buffer were added in duplicates to each well. For the unknown samples, 22.5µl of the same SDS buffer and 2.5µl of each sample were added to each well to establish a 1:10 dilution. 200µl of the assay solution were then added to each well, followed by incubation at 37°C for 30 minutes. The assay solution was prepared by adding one volume of 4.0% $CuSO_4$ (Reagent B, provided in the Kit) to 50 volumes of the Bicinchoninic Acid solution (Reagent A, provided in the kit). After incubation, the absorbance of each well was read with a spectrophotometer (BIOTEK Power 200) at 562nm.

***Antibodies*** - The following antibodies were used in this study: anti-c-myc (A-14) rabbit polyclonal that recognizes the 9E10 c-Myc tag (1:2,000 from Santa Cruz Biotechnology, Inc., CA), anti-ubiquitin conjugates rabbit polyclonal (1:1,500 from Dako Corp., CA) and anti-20S proteasome (1364) rabbit polyclonal antibody raised against whole 20S proteasomes purified from mouse spleen and liver (a generous gift from Dr. J. Monaco, Cincinnati, OH).

***Western Blotting and Non-denaturing Polyacrylamide Gel Electrophoresis (PAGE)*** - Total lysates of HT4 cells were subjected to SDS-PAGE (12% gels for detection of 20S proteasome subunits and 8% gels for detection of ubiquitin-protein conjugates) and 10 - 20μg of protein were loaded per lane. Antigens were visualized using the Supersignal West PICO chemiluminescent substrate (Pierce, IL). Protein bands were semi-quantified with the Scion Image program (NIH, Bethesda, MD). For non-denaturing analysis of the 20S proteasome, total lysates of HT4 cells prepared in 0.01mM Tris/EDTA, pH7.5 in the absence of SDS, were run on non-denaturing 4% polyacrylamide gels followed by immunoblotting analysis with the anti-c-myc antibody. 50μg of total protein from vector and MC13-c-myc stable transfectants and 250μg of total protein from Muta-1-c-myc stable transfectants were loaded per lane. Purified native bovine pituitary 20S proteasome (6μg) was run in a parallel lane, which was excised prior to Western blotting and was stained with Coomassie blue.

***Immunoprecipitation*** - After normalizing for protein concentration, immunoprecipitations were carried-out in a

0.01M Tris-EDTA, pH 7.5 buffer with mouse anti-c-myc monoclonal antibody agarose beads that recognize the 9E10 Myc tag (BD Biosciences, CA). The anti-c-myc agarose beads were first washed three times with 0.01M Tris-EDTA, pH 7.5 buffer. Enough buffer was added to the beads to make a 1:1 bead slurry. 60µl of this bead slurry were added to each tube containing the cell lysates and the mixtures were incubated at 4°C overnight with light rotation. In the following day, antigen-antibody complexes coupled with agarose beads were spun down and washed twice with the 0.01M Tris-EDTA, pH 7.5 buffer. The immunocomplexes were then eluted and resolved on 12% SDS PAGE, followed by Western blot analysis probed with anti-c-myc antibody.

***Measurement of 20S proteasome chymotrypsin-like activity*** - Proteasome activity was assessed in normalized supernatant and pellet fractions of immunoprecipitation assays. The 20S proteasome particles that incorporated the c-myc tagged β5 subunits were immunoprecipitated under native conditions from total cell lysates with anti-c-myc agarose beads in a 0.01M Tris-EDTA, pH 7.5 buffer. The anti-c-myc agarose beads in the pellet fractions were washed twice with the same 0.01M Tris-EDTA, pH 7.5 buffer prior to addition of the chymotrypsin-like activity

substrate succinyl-LLVY-methylcoumarylamide (BACHEM Bio-science, Inc., PA). The peptidase activity was assayed colorimetrically (Wilk and Orlowski, 1983) after 24h incubations at 37°C.

***Cell viability Assay*** - Cell viability was assessed by a modified Mosmann's method (Mosmann, 1983). 3-(4, 5-dimethylthia-zol-2-yl)-2, 5-diphenyl tetrazolium bromide (MTT) at a final concentration of 0.5mg/ml was dissolved in the HT4 cell culture media containing 5% fetal bovine serum. The incubation media of HT4 cells grown in 24-well plates was removed and the cells in each well were incubated with 0.5ml of the MTT solution for 1h at 37°C in 5% $CO_2$. The supernatant was aspirated and 0.4ml of a solution of 0.04M HCL in isopropanol were added and gently shaken to dissolve the precipitated formazan dye. The plates were centrifuged at 5,000g for 5 minutes and the absorbance of the supernatant was read at 550nm and 620 nm with a spectrophotometer (BIOTEK Power 200). The results were expressed as the difference between the values obtained at the two wavelengths.

***Immunocytochemistry*** - After fixation with a 1% formaldehyde solution in Dulbecco's modified Eagle's

medium, cells were immunostained with the anti-ubiquitin conjugate antibody at a dilution of 1:500. Immunoreactivity was detected with the ABC kit (Vector Laboratories, CA) following a protocol provided by the manufacturer with DAB/$H_2O_2$ as a brown chromogen. Cells were counterstained with hematoxylin, which revealed cell nuclei as blue circular structures.

***Statistical Analysis*** - Statistical significance was estimated using one-way ANOVA with the Tukey-Kramer multiple comparison test with *$p<0.01$ for differences between control and cadmium-treated cells.

***Generation of Transgenic Mice*** - Sequences corresponding to the human CMV promoter, c-myc tagged MC13/Muta-1 and the SV40 polyadenylation signal were released from the plasmid backbone using a combination of *MfeI* and *NaeI*. DNA containing this expression cassette was purified from an agarose slice by electroelution, followed by phenol/chloroform extraction and ethanol precipitation. The purified DNA was microinjected into male proneuclei of FVB mouse fertilized eggs, which were cultured to the two-cell stage and implanted into pseudopregnant CD-1 female recipients. This method is routinely used by the transgenic

mouse facility at Albert Einstein College of Medicine (Lab director: Dr. Chen).

***Screening of the Transgenic Mouse Lines*** - Approximately 10mm long fragments of mouse tails were excised from the tip region. The fragments were digested with proteinase K at 55°C overnight. On the following day, the genomic DNA from tail fragments was purified with a Dneasy® Tissue Kit (Qiagen, CA). The primers used for Polymerase Chain Reaction (PCR) were the T7 (forward) primer and Bovine Growth Hormone (BGH) Reverse primer from the pcDNA3.1/hygro(-) vector (Invitrogen, CA). The sequence of the T7 primer was: 5'TAATACGACTCACTATAGG-G3' and the sequence of BGH Reverse primer was: 5'TAGAAGGCACAGTCGAGG3'. PCR reactions were set-up as follows: 95°C for 10min, then 35 cycles at 95°C for 1min, 55°C for 2min and 72°C for 3min, with a final extension at 72°C for 10min. To distinguish the Muta-1-c-myc from the MC13-c-myc PCR fragments, the amplified sequences were subjected to restriction analysis with *SfoI* or *Bam HI*.

# *Chapter III*

# Results

**1. Mutation of Thr1 to Ala1 in MC13 - the β5 subunit of the mouse 20S proteasome.**

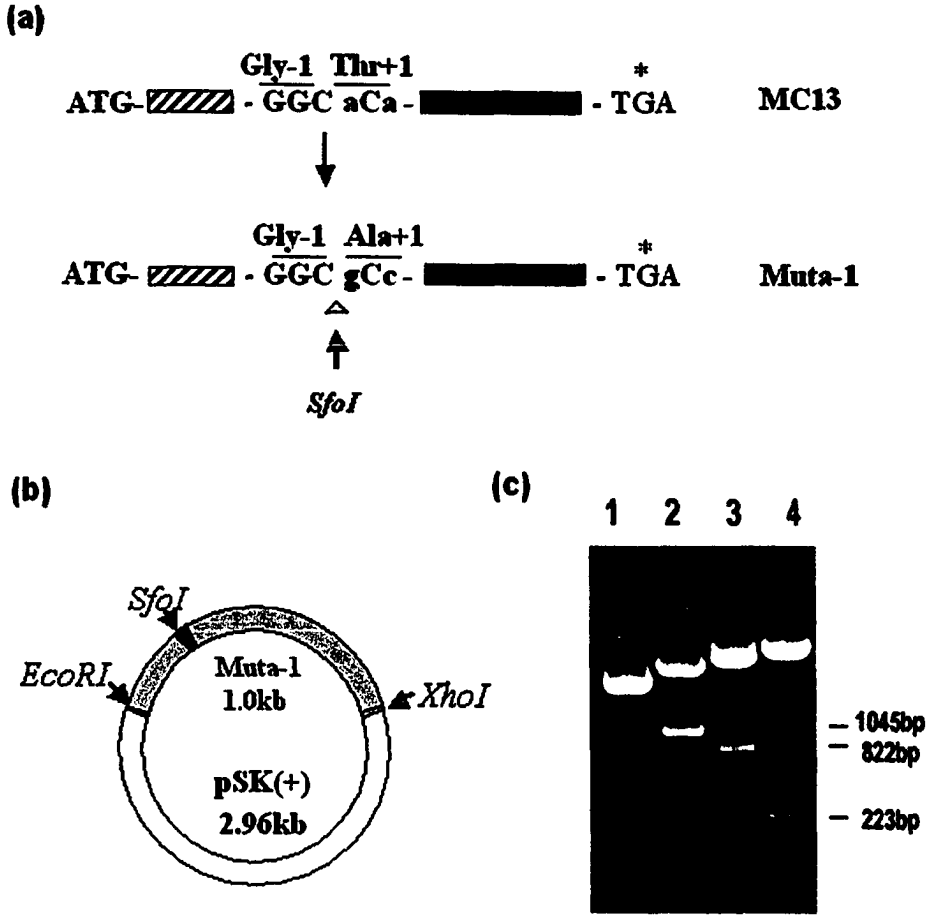


**Figure 3.1 - Mutation of Thr1 to Ala1 in MC13 - (a)** Schematic of the β5 constructs showing the relative positions of the start codon "ATG", precursor pro-peptide (hatched box), the mature β5 subunit (dark gray filled box) and the stop codon "TGA*". The two mutated base pairs (**a** to **g** and **a** to **c**) are in lower case and bold and indicate a sequence change that introduces a unique *Sfo1* site. Amino acid numbers refer in all cases to positions relative to the mature β5 subunit. **(b)** Schematic of the restriction sites for the three enzymes, *EcoRI*, *XhoI* and *SfoI*, on the *Muta-1* construct cloned in pScriptBlue SK(+) vector. **(c)** Restriction analysis of *Muta-1* cloned into the pScriptBlue SK(+) vector. 1-uncut. 2-*EcoRI/XhoI* digestion (the size of the *Muta-1* insert is 1.045kb). 3-*SfoI/XhoI* digestion (a 822bp fragment was produced). 4-*EcoRI/SfoI* digestion (a 223bp fragment was produced).

The MC13 cDNA was originally cloned into an *EcoRI* site on a pBluescriptSK(+) vector (Stratagene, CA). In the current study, the N-terminal threonine of the mature MC13 subunit of the mouse 20S proteasome was mutated to alanine with the Site-directed Mutagenesis Kit from Stratagene®. The two mutated base pairs (**a** to **g** and **a** to **c**) are shown in lower case and bold (Figure 3.1a). The mutated MC13 subunit was designated as Muta-1. Concomitantly, a unique *Sfo1* restriction site was introduced upstream of the mutated codon encoding Ala1, to be able to distinguish wild type (*MC13*) and mutant (*Muta-1*) forms of the β5 gene by restriction analysis (Figure 3.1b and 3.1c). Amino acid numbers refer in all cases to positions relative to the mature MC13 subunit.

**2. Subcloning of MC13 and Muta-1 into a mammalian expression vector.**

The MC13 and the Muta-1 cDNAs were subcloned into the pcDNA3.1/hygro(-) mammalian expression vector (Invitrogen, CA). This vector contains an immediate-early human cytomegalovirus (CMV) promoter, a multiple cloning site, a polyA signal, the ampicillin resistance gene to allow

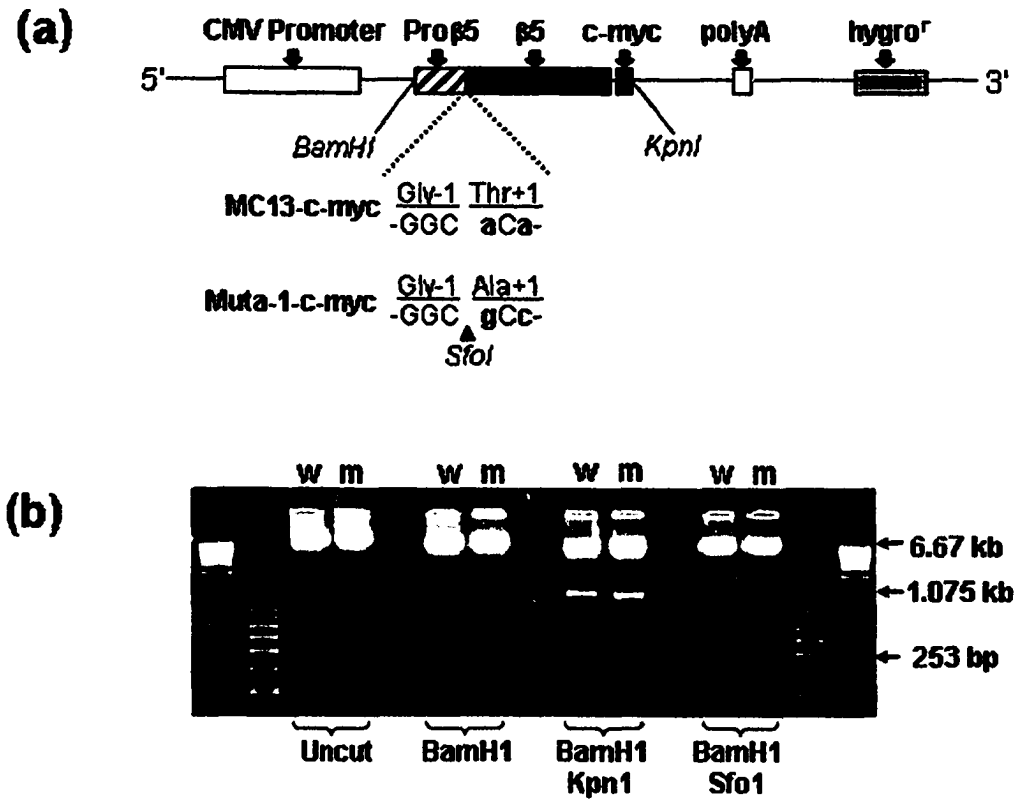


**Figure 3.2 - Restriction analysis of *β5-c-myc* subcloned in pcDNA3.1/hygro (-) vector.** **(a)** Schematic of the β5 constructs showing the relative positions of the CMV promoter (open box), the precursor pro-peptide (Proβ5, hatched box), the mature β5 subunit (β5, dark gray filled box), the c-myc tag (c-myc, black box), the polyA signal (poly A, open box) and the hygromycin-resistance gene (hygro$^r$, light gray filled box). The two mutated base pairs (**a** to **g** and **a** to **c**) are in lower case and bold and indicate a sequence change that introduces a unique *SfoI* site. Amino acid numbers refer in all cases to positions relative to the mature β5 subunit. **(b)** Restriction analysis of subcloned *MC13-c-myc* (w) and *Muta-1-c-myc* (m) genes. The size of the *β5-c-myc* gene is 1.075kb. A 253bp fragment was produced by *BamHI/SfoI* double digestion of the mutant construct and not of the wild type.

selection in bacteria and the hygromycin resistance gene to allow selection in mammalian cells (Figure 3.2a). In addition, for detection, a *c-myc* tag was introduced at the C-terminus of *MC13* or *Muta-1* to distinguish between exogenously expressed and endogenous MC13 subunits. The *c-myc* tag was specifically chosen because it consists of a short stretch of amino acids (EQKLISEEDL) and is less charged than other widely used epitope tags, such as *FLAG* and *hemagglutinin*, which may interfere with the function or assembly of the MC13 subunit into the 20S proteasome particle. The final constructs obtained from this subcloning are shown in Figure 3.2a. Both *MC13-c-myc* and *Muta-1-c-myc* were ligated into the *BamHI* and *KpnI* sites in the pcDNA3.1/hygro(-) vector. Subcloning and mutations were verified by DNA sequencing (data shown in APPENDIX) and restriction analysis (Figure 3.2b). The size of the *MC13-c-myc* insert is 1.075kb. A 253bp fragment was produced by *BamH1/Sfo1* double digestion of the mutant construct but not of the wild type construct, thus confirming the effectiveness of the site directed mutagenesis.

**3. Transiently expressed MC13-c-myc and Muta-1-c-myc are not incorporated into the mouse 20S proteasome particle in HT4 cells.**

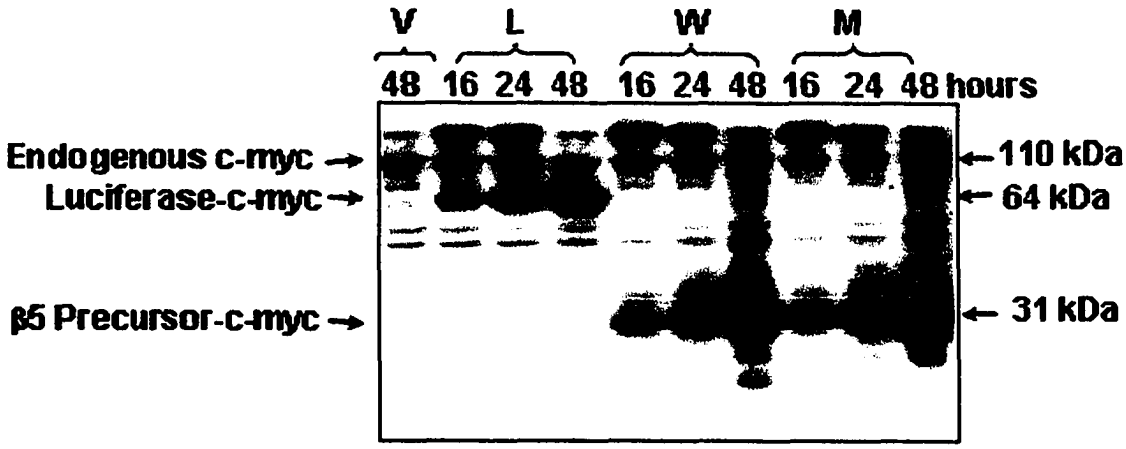


**Figure 3.3 - Transient expression of the mutant β5 subunit in mouse neuronal HT4 cells.** Western blot analysis of HT4 cells transiently transfected with vector (V), *Luciferase-c-myc* (L), *MC13-c-myc* (W) or *Muta-1-c-myc* (M). Cells were harvested 16, 24 or 48 hours after transfection. Immunoblots were probed with anti-c-myc antibody. Molecular mass markers are on the right.

To assess the expression levels of the subcloned 20S proteasome β5 subunits *in vivo*, MC13-c-myc and Muta-1-c-myc fusion proteins as well as a luciferase-c-myc positive control were transiently expressed in mouse neuronal HT4 cells. Western blot analysis with an anti-c-myc antibody detected MC13-c-myc, Muta-1-c-myc and luciferase/c-myc

expression 16, 24 and 48h after transfection (Figure 3.3). The β5 fusion proteins were detected as ~31kDa c-myc tagged precursors and not as mature MC13-c-myc or Muta-1-c-myc proteins, whereas endogenous c-myc was detected as an 110kDa protein (Figure 3.3). The MC13 subunit is first synthesized as a precursor protein (mouse MC13 precursor ~30.2kDa, c-myc tag ~1.2kDa) and the N-terminal propeptide is required for incorporation into the 20S proteasome particle (Kruger and Enenkel, 2001). Once the particle is fully assembled, the propetide is autocatalytically removed to produce the mature, catalytically active MC13 subunit of an expected molecular weight of 22.7kDa. Since the half-life of the mammalian 20S proteasome is 12-15 days (Tanaka and Ichihara, 1989), the experimental time of up to 48h was not long enough to allow integration of the transiently expressed β5 subunits into newly assembled 20S proteasome particles and, therefore, they were not processed to the mature forms. Given these findings and the demonstration that the expression levels of the β5 fusion proteins decreased dramatically 72h after transfection, stable transfectants expressing the MC13-c-myc, Muta-1-c-myc and the empty vector were prepared by selection for hygromycin B resistance.

**4. Differential processing of MC13-c-myc and Muta-1-c-myc stably expressed in HT4 cells.**

MC13-c-myc and Muta-1-c-myc expressing stable colonies were screened for subunit expression by Western blot

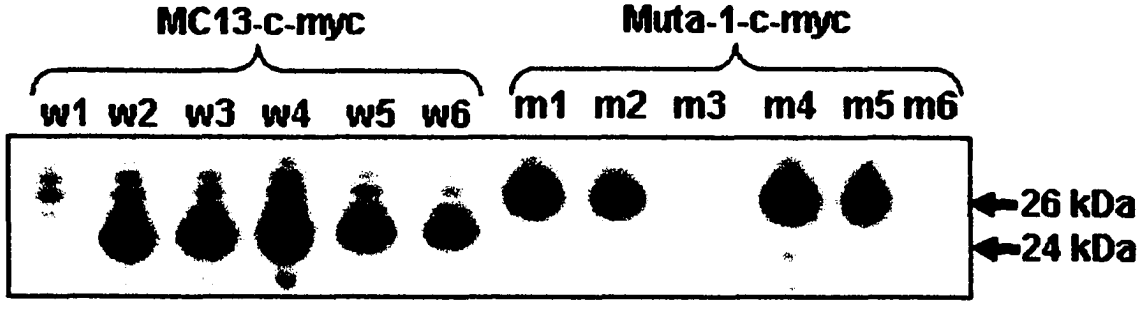


**Figure 3.4 - Differential processing of MC13-c-myc and Muta-1-c-myc stably expressed in HT4 cells.** MC13-c-myc (lanes w1 to w6) or Muta-1-c-myc (lanes m1 to m6) stable clones screened for subunit expression by Western blot analysis with the anti-c-myc antibody.

analysis with the anti-c-myc antibody. As shown in Figure 3.4, not all colonies exhibited similar expression levels of the respective fusion proteins. This effect was most likely due to damage of the constructs during the incorporation events. MC13-c-myc was detected as a ~24kDa band, corresponding to the autocatalytically processed,

mature MC13 subunit (22.7kDa) tagged with c-myc (1.2kDa) at the C-terminus. Maturation of the MC13 subunit is a process that takes place subsequent to incorporation into the 20S proteasome particle. In mammals, maturation of β subunits is a two-step autocatalysis where an intact Gly-1/Thr+1 consensus motif coupled to Lys33 are essential for correct processing in which Thr1 acts as the nucleophile and Lys33 as the proton donor/acceptor (Schmidtke et al., 1996).

Since Thr+1 was replaced by Ala+1 in the mutant MC13 subunit (Muta-1), precursor processing occurred at a non-canonic site producing a c-myc tagged mutant protein that was detected as a ~26kDa band (Figure 3.4). This larger size corresponds to a misprocessed Muta-1 subunit with an extended 2.1kDa N-terminal sequence that resides upstream from the Thr1Ala mutation site. Our findings with the mouse Muta-1 subunit are in agreement with reports of similar mutations in the yeast β5 (PRE2) (Chen and Hochstrasser, 1996) and human inducible β1i (LMP2) subunits (Schmidtke et al., 1996). These studies demonstrated that the N-terminal extension of the mutant subunits does not interfere with the correct assembly of the 20S proteasome particle.

**5. Stably expressed MC13-c-myc and Muta-1-c-myc are incorporated into the 20S proteasome particle.**

Immunoprecipitation under native conditions with mouse monoclonal anti-c-myc agarose beads or with an anti-proteasome antibody used to purify intact mouse 20S proteasomes (Beyette et al., 2001) pulled down mostly the processed forms of MC13-c-myc and Muta-1-c-myc, attesting to their incorporation into the quaternary structure of the 20S proteasome (Figure 3.5a). A small fraction of unprocessed fusion proteins was immunoprecipitated with the anti-c-myc agarose beads only. Incorporation of β5-c-myc subunits into the 20S proteasome particle was further confirmed by non-denaturing PAGE of total extracts from stable transfectants analyzed by immunobloting with the anti-c-myc antibody (Figure 3.5b). A c-myc immunoreactive band corresponding to the 20S proteasome particle was only

detected in the lanes loaded with extracts from MC13-c-myc (WT) and Muta-1-c-myc (M) stable transfectants. The position of the non-denatured 20S proteasome particle was

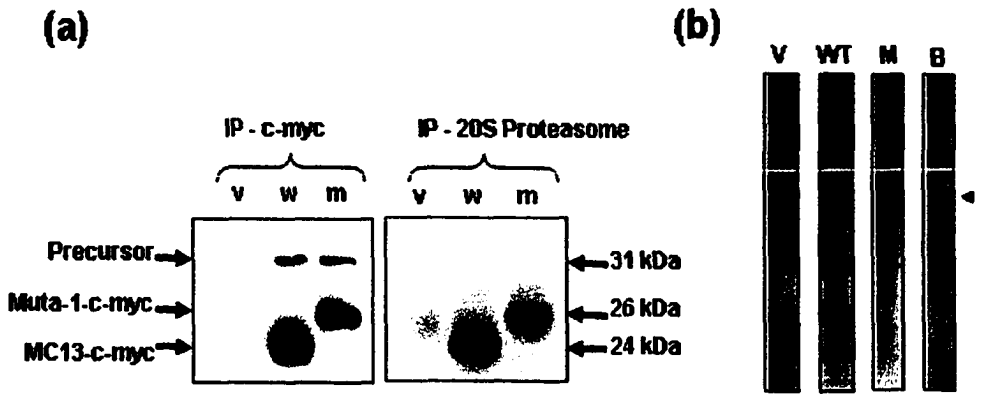


**Figure 3.5 - The wild type and mutant β5 subunits are both incorporated into the quaternary structure of the 20S proteasome.** **(a)** 20S proteasome immunoprecipitated under native conditions from total lysates of stable transfectants expressing vector (v), MC13-c-myc (w) or Muta-1-c-myc (m) with anti-c-myc agarose beads (left panel) or with an anti-20S proteasome antibody used to immunopurify intact 20S proteasome (right panel). Immunoblots of the precipitated proteins were probed with the anti-c-myc antibody. Molecular masses are on the right. **(b)** Non-denaturing PAGE of extracts from stable transfectants expressing vector (V), MC13-c-myc (WT) and Muta-1-c-myc (M) followed by anti-c-myc immunoblot analysis. (B) Native 20S proteasome (6μg) purified from bovine pituitaries run in a parallel lane of the non-denaturing gel followed by staining with Coomassie blue. The position of the 20S proteasome particle is indicated by an arrow. One unidentified wide protein band that cross-reacted with the anti-c-myc antibody was apparent in the WT lane.

verified by running 6μg of native 20S proteasome purified from bovine pituitaries in a parallel lane of the non-denaturing gel. This lane was excised prior to Western blot analysis of the remainder of the gel and the purified 20S proteasome was detected by Coomassie blue staining (Figure 3.5b).

**6. Incorporation of Muta-1-c-myc into the mouse 20S proteasome inhibits its chymotrypsin-like activity.**

The chymotrypsin-like activity of 20S proteasome particles containing c-myc tagged β5 subunits was evaluated with the substrate succinyl-LLVY-methylcoumarylamide. For these experiments, 20S proteasome particles containing MC13-c-myc and Muta-1-c-myc were affinity purified in "pull-down" assays by immunoprecipitation of stable transfectant lysates with anti-c-myc agarose beads under native conditions. The affinity purified MC13-c-myc containing 20S proteasome particles were found to be

catalytically active as demonstrated by the level of hydrolysis of the succinyl-LLVY methylcoumarylamide

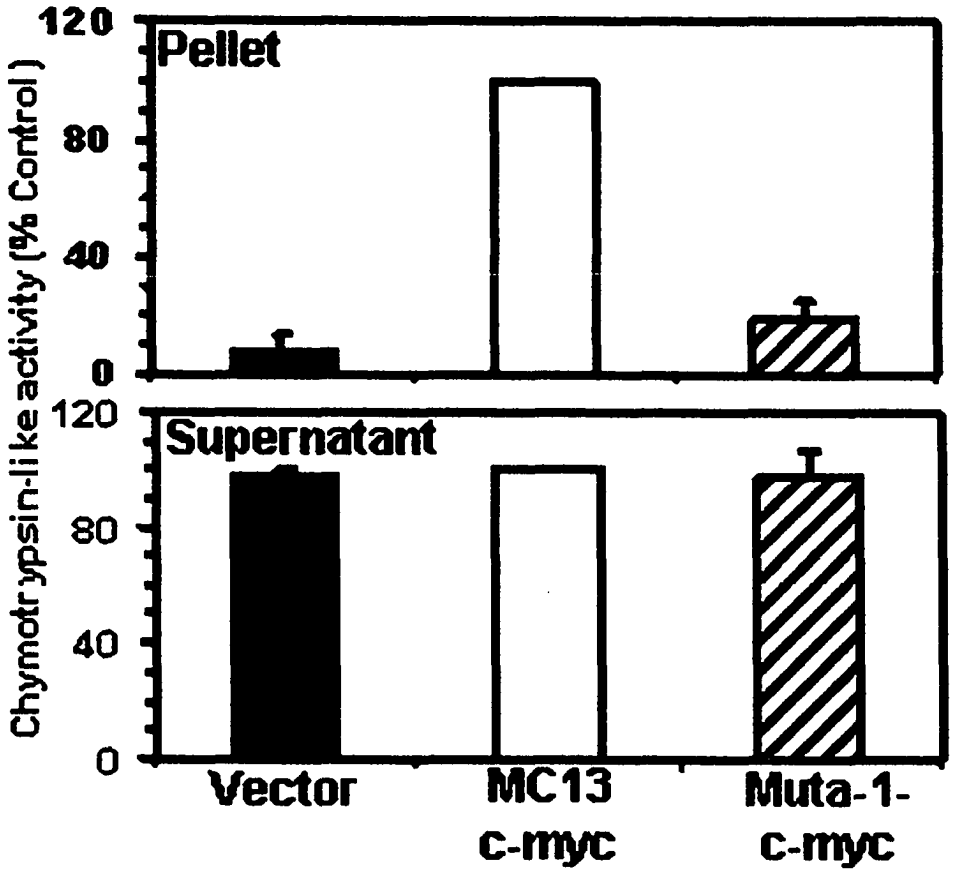


**Figure 3.6 - Mutant (T1A) β5 subunits impair the chymotrypsin-like activity of the 20S proteasome.** Chymotrypsin-like activity of proteasomes immunoprecipitated under native conditions from total lysates of stable transfectants expressing vector (full bars), MC13-c-myc (open bars) or Muta-1-c-myc (hatched bars). Chymotrypsin-like activity was measured in pellet (top graph) as well as in supernatant (bottom graph) fractions. Results are expressed as percentage of MC13-c-myc clones. Values represent the mean of three independent experiments and error bars indicate the SEM.

substrate (Figure 3.6). Since expression of Muta-1-c-myc produced β5 subunits without the active site Thr+1, affinity purified Muta-1-myc containing 20S proteasomes displayed an 80% reduction in chymotrypsin-like activity (Figure 3.6). The residual 20% activity detected in the Muta-1-c-myc pellet fractions most likely represents chymotrypsin-like activity of hybrid 20S proteasome particles each containing one endogenous MC13 and one cloned Muta-1-c-myc subunit. Immunoprecipitates of "vector" stable transfectants with the anti-c-myc agarose beads displayed very low chymotrypsin-like activity as expected (Figure 3.6). The supernatant fractions from the affinity purification exhibited similar levels of chymotrypsin-like activity, as they contained mostly 20S proteasome particles with endogenous, untagged MC13 subunits (Figure 3.6).

**7. 20S proteasomes with Muta-1-c-myc hypersensitize HT4 cells to cadmium-induced oxidative stress.**

HT4 cells are a mouse neuroblastoma cell line immortalized with a recombinant temperature sensitive mutant of the SV40 large T antigen (Whittemore et al.,

1991). Stocks are maintained at the permissive 33°C temperature. When transferred to 39°C (non-permissive temperature), their growth rate is significantly decreased and they differentiate with a neuronal phenotype (Whittemore et al., 1991). At the 33°C permissive temperature the Muta-1-c-myc stable clones exhibited a slightly slower growth rate than vector and MC13-c-myc stable transfectants. This was expected, as proteasome inhibition is known to block cell proliferation especially in dividing cells (Goldberg and Rock, 2002). However, growth rates of vector, wild type and mutant stable clones maintained under homeostatic conditions (37°C) following differentiation at the non-permissive 39°C temperature, were similar and the different clones were morphologically indistinguishable.

We next compared the vulnerability of MC13-c-myc and Muta-1-c-myc stable transfectants to oxidative stress. We treated the stable transfectants with cadmium as our model oxidative stressor because the heavy metal does not affect the peptidase activities of the 20S proteasome (Figueiredo-Pereira and Cohen, 1999) and thus does not interfere with the effect of the Muta-1-c-myc. To assess the effects of

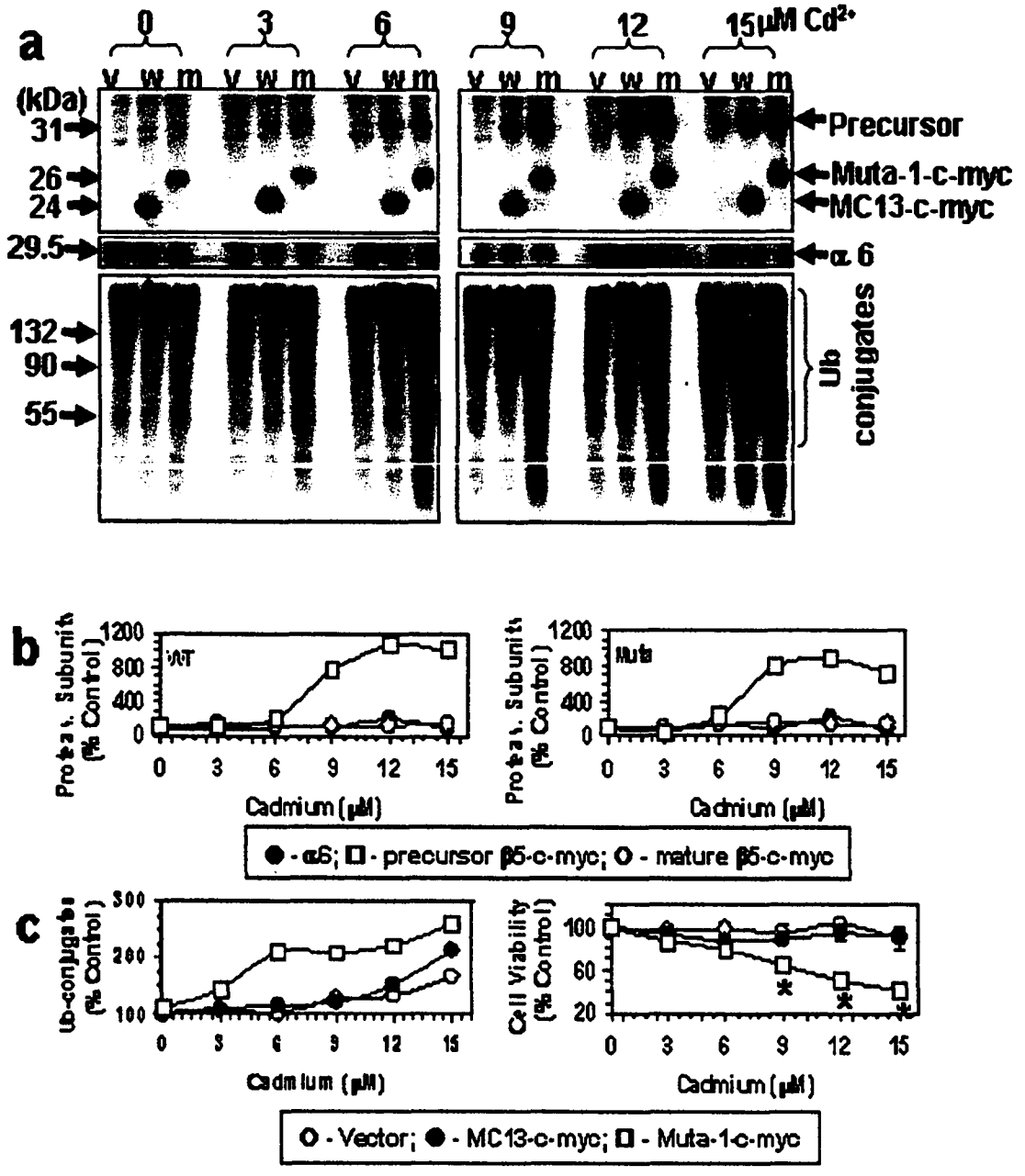


**Figure 3.7 - Expression of Muta-1-c-myc hyper-sensitizes cells to oxidative stress -** Stable transfectants expressing vector (v), MC13-c-myc (w) and Muta-1-c-myc (m) were exposed to increasing concentrations of cadmium ($Cd^{2+}$) for 24hr. **(a)** Expression levels of the cloned β5 subunits (top panel) were assessed by Western blot analysis with the anti-c-myc antibody. Equal protein loading was demonstrated by reprobing the same blot with the anti-α6 antibody (middle panel). High molecular weight ubiquitin-protein conjugates (Ub conjugates) were detected by Western blotting probed with the anti-ubiquitin-conjugate antibody (lower panel).

**Figure 3.7 (continuation) (b)** Semi-quantification of precursor (□) or mature (O) forms of β5-c-myc and α6 (●) in wild type (left graph) and mutant (right graph) stable transfectants detected in (a). **(c, left graph)** Semi-quantification of ubiquitinated protein levels in vector (O), wild type (●) or mutant (□) stable transfectants detected in (a). **(c, right graph)** Cell viability of vector (O), wild type (●) and mutant (□) stable transfectants. Results are expressed as percentage of untreated cells for each clonal line. Each point is the mean of three independent experiments and error bars indicate the SEM. Statistical significance was estimated using one-way ANOVA with the Tukey-Kramer multiple comparison test with *$p<0.01$ for differences between control and cadmium-treated cells.

oxidative stress, the mouse neuronal HT4 stably transfected cells were treated with cadmium only after the differentiated cells were maintained at 37°C for 24h in the absence of hygromycin B. Western blots of total lysates from stable transfectants expressing vector alone, MC13-c-myc or Muta-1-c-myc were probed with an anti-ubiquitin conjugate antibody (Figure 3.7a, bottom panel). In the absence of cadmium, no significant accumulation of ubiquitinated proteins was detected. However, an approximate 2- to 2.5-fold increase in ubiquitin-protein conjugate levels was observed in Muta-1-c-myc stable transfectants treated with cadmium concentrations as low as 6μM (Figure 3.7a, bottom panel; Figure 3.7c, left panel). Accumulation of ubiquitinated proteins was detected in

vector or MC13-c-myc stable transfectants only when these cells were treated with much higher (15μM) cadmium concentrations (Figure 3.7a, bottom panel; Figure 3.7c, left panel).

No decreases in cell viability were elicited by the heavy metal on cells expressing vector or MC13-c-myc (Figure 3.7c, right panel). However, Muta-1-c-myc stable transfectants displayed significant decreases in cell viability (Figure 3.7c, right panel) in response to cadmium treatment at concentrations as low as 9μM. These results indicate that a moderate impairment of the 20S proteasome activity, as the one exhibited by the Muta-1-c-myc stable transfectants, can drastically hypersensitized the neuronal cells to oxidative stress.

Precursor levels of MC13-c-myc and Muta-1-c-myc rose to a maximum of 11-fold above control with increasing concentrations of cadmium (Figure 3.7a, top panel; Figure 3.7b). This response most likely reflects the cadmium-mediated activation of the human cytomegalovirus (CMV) immediate-early promoter present in the pcDNA3.1/Hygro(-) vector (Beyersmann and Hechtenberg, 1997). These results also indicate that the excess precursors were not

processed, probably due to a shortage of proteasome subunits other than β5, necessary to assemble additional 20S proteasome particles. This is confirmed by the finding that the levels of the α6 proteasome subunit were not altered by cadmium, as judged by Western blot analysis and a semi-quantification of the results (Figure 3.7a, middle panel; Figure 3.7b). The levels of mature MC13-c-myc and Muta-1-c-myc also did not change considerably in the cadmium treated cells compared to untreated controls (Figure 3.7a, top panel; Figure 3.7b).

The level of 20S proteasome mutant particles was always lower than that of wild type particles, as judged by comparing the intensities of the bands corresponding to misprocessed Muta-1-c-myc (26kDa) and mature MC13-c-myc (24kDa) (Figure 3.7a, top panel). In addition, the lower levels of misprocessed Muta-1-c-myc subunit appear to correlate with the higher amounts of its precursor. These results suggest that the mutant particles are structurally unstable and that less of the misprocessed Muta-1-c-myc subunit is incorporated into the 20S proteasome particle. This notion is supported by the fact that four-fold more protein from Muta-1-c-myc than from MC13-c-myc stable transfectant lysates had to be loaded onto the non-

denaturing gel lanes to detect the respective c-myc tagged 20S proteasome particles (Figure 3.5b). Similar results were obtained when an identical mutation was expressed in yeast (Chen and Hochstrasser, 1996). The mutant yeast 20S proteasome particles were found to be unstable and the levels of mutant precursor were also increased when compared to wild type. This mutation was not lethal but it hypersensitized the yeast strains to L-canavanine and to storage at 4°C (Chen and Hochstrasser, 1996).

**8. Muta-1-c-myc stable transfectants display large ubiquitin conjugate aggregates under oxidative stress conditions.**

The occurrence of intracellular inclusions containing ubiquitinated proteins is a hallmark of neurodegeneration but the mechanisms leading to inclusion formation and their relationship to neurodegeneration are not clear. Nevertheless, the involvement of ubiquitin in neurodegeneration is so generally accepted that ubiquitin immunoreactivity is used regularly in the identification of pathological lesions, such as Lewy Bodies and

Neurofibillary Tangles (NFT) that are associated with neurodegenerative disorders. We investigated whether reduced 20S proteasome activity alone can lead to the formation of intracellular inclusions containing ubiquitinated proteins. No ubiquitin immunoreactive inclusions were detected in vector, MC13-c-myc and Muta-1-c-myc grown under control conditions. These results indicate that, under homeostatic conditions, a decrease in proteasome activity is not sufficient to induce inclusion formation. However, Muta-1-c-myc stable transfectants treated with 9μM cadmium for 24hrs at 37°C exhibited large ubiquitin-protein aggregates detected by immunocytochemistry with the same anti-ubiquitin antibody employed in the Western blot analysis (Figure 3.8f). Some of the largest ubiquitin-protein aggregates caused nuclear distortions (Figure 3.8g and h) similar to those found in Lewy body containing neurons. Most of vector and MC13-c-myc stable transfected cells treated with 9μM cadmium exhibited mostly small ubiquitin-protein aggregates (Figure 3.8d and e), although large aggregates could also be detected in a

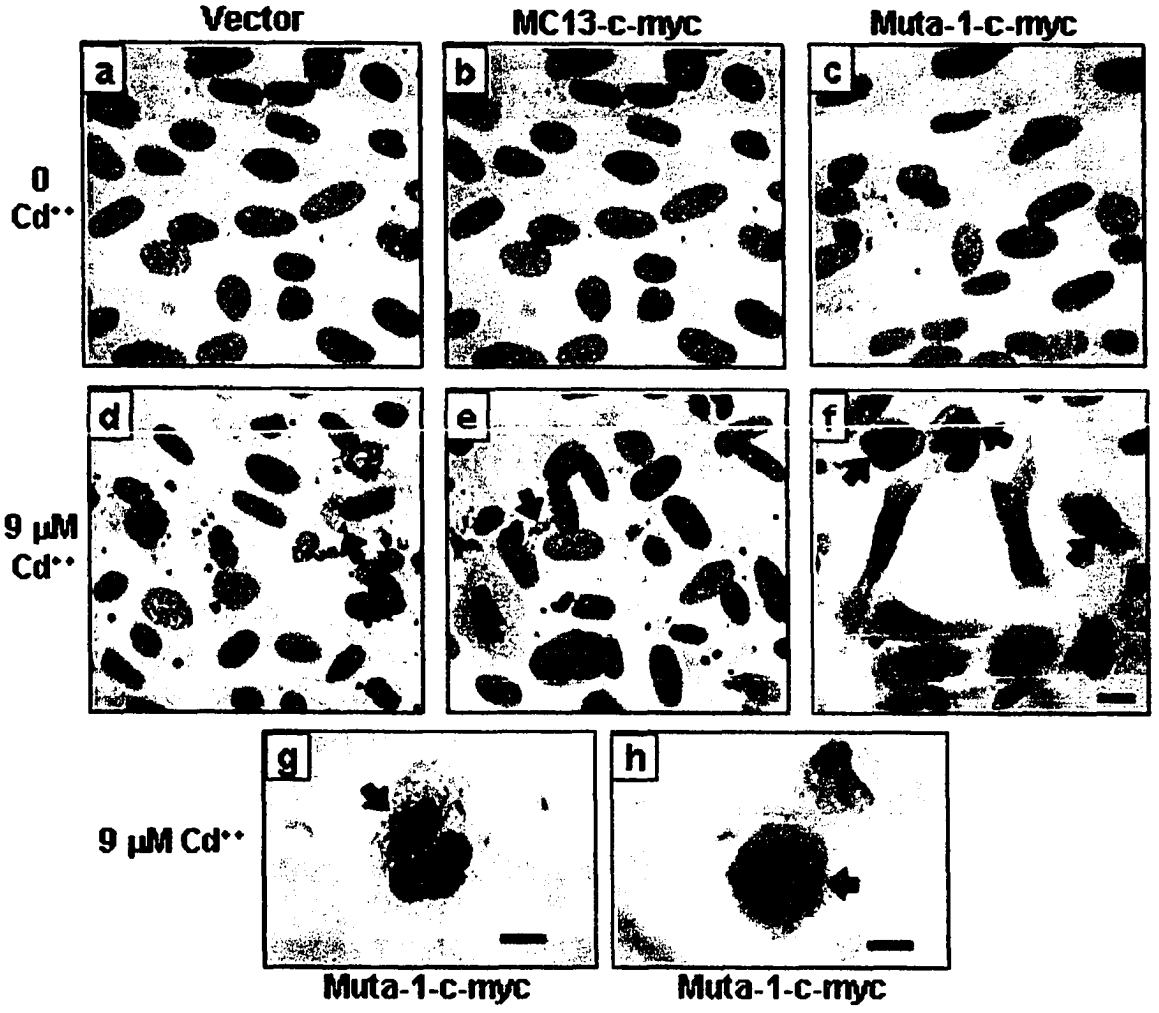


**Figure 3.8 - Accumulation of ubiquitin-protein conjugates in aggregates** - Vector (d), MC13-c-myc (e) and Muta-1-c-myc (f-h) stable transfectants were treated for 24hr with 9µM cadmium. Aggregated ubiquitinated proteins (arrows) were visualized with the anti-ubiquitin conjugate antibody by a standard Vector ABC immunostaining protocol with DAB/$H_2O_2$ as a brown chromogen. No ubiquitin-protein aggregates were detected in untreated vector (a), MC13-c-myc (b) and Muta-1-c-myc (c) stable transfectants. Counterstaining with hematoxylin revealed round blue nuclei. Scale bars represent 10µm in **a-f** and 6.6µm in **g** and **h**.

few of these cells. These results indicate that neuronal cells exhibiting a decrease in proteasome activity are more prone to developing inclusions when subjected to oxidative stress, than normal cells.

**9. Transgenic mouse lines expressing MC13-c-myc or Muta-1-c-myc.**

These studies were carried-out in collaboration with Dr. Peter Werner from the Albert Einstein College of Medicine in New York.

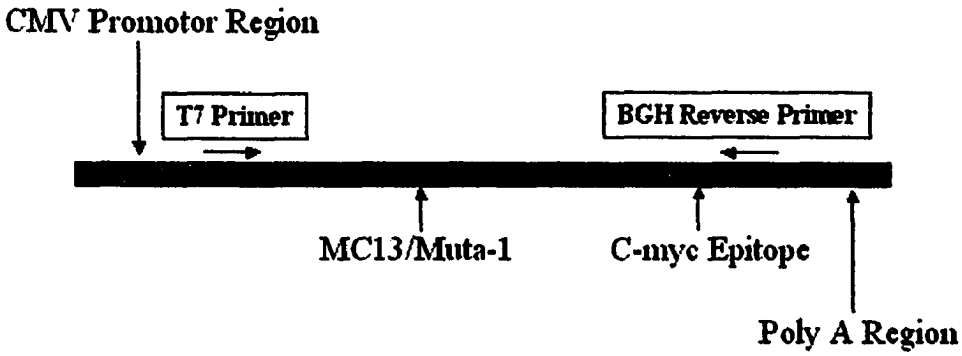


**Figure 3.9 - Transgenesis construct.** Schematic of the β5 construct for transgenic mice showing the relative positions of the CMV promoter, the precursor β5 subunit (MC13/Muta-1), the c-myc tag and the polyA signal. The two vector-derived primers used for PCR analysis, T7 and BGH reverse, will hybridize with the flanking regions of the MC13-c-myc/Muta-1-c-myc insert.

To create an experimental animal model for progressive neurodegeneration associated with proteasome dysfunction, transgenic mice displaying widespread expression of MC13-c-myc and Muta-1-c-myc were generated. The full-length constructs for transgenesis are shown in Figure 3.9. To screen for positive transgenic mice, vector-derived T7 and BGH Reverse primers, which hybridize with the flanking regions of the constructs, were used in PCR reactions.

From 134 injected fertilized eggs, a total of twelve independent transgenic founders were obtained: seven

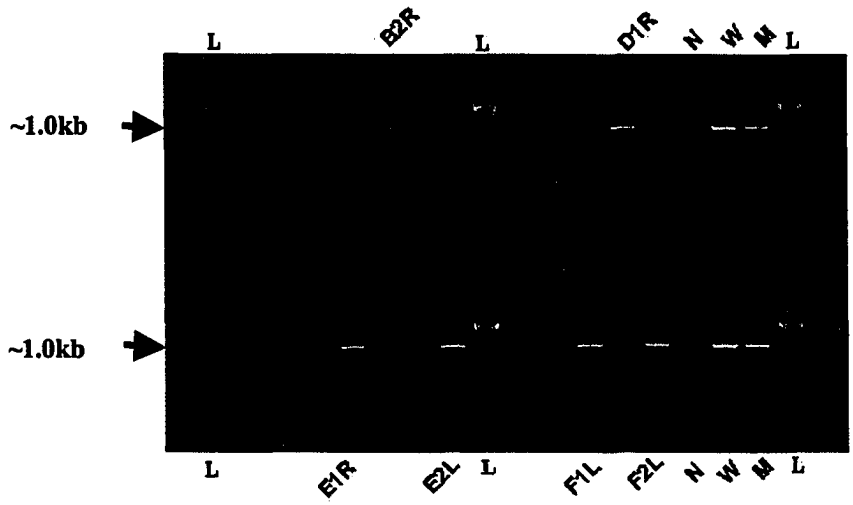


**Figure 3.10 - PCR screening for transgenic mouse founders.** 20µl of each PCR reaction mixture were resolved on a 2% agarose gel. B2R, D1R, E1R, E2L, F1L and F2L are ID numbers for mice showing the positive results. "L"- 500bp DNA ladder (BioRad, CA). "N"- negative control; "W"- MC13-c-myc in the pcDNA3.1/hyfro(-) vector; "M"- Muta-1-c-myc in the pcDNA 3.1/hygro(-) vector.

expressing MC13-c-myc and five expressing Muta-1-c-myc. Figure 3.10 shows the ~1.0kb PCR products resulting from PCR amplification of tail DNA obtained from the respective founders. A negative control with no template (N) and two positive controls, MC13-c-myc (W) and Muta-1-c-myc (M) subcloned into the pcDNA3.1/hygro(-) vector, were run in parallel lanes on the agarose gel. The positive controls indicate the expected size of the PCR products.

Mutant and wild type transgenic mice were genetically distinguishable by restriction analysis with *BamHI* or *SfoI* of the PCR products obtained from tail DNA. Due to the introduction of a *SfoI* restriction site by site-directed mutagenesis of the MC13 cDNA, *SfoI* digestion of PCR products from mutant pups yielded two bands: a 690bp band and a 373bp band (Figure 3.11). Since there is no *SfoI* restriction site within the *MC13-c-myc*, *SfoI* digestion of PCR products from wild type pups produced a 1063bp band, which corresponds to the uncut PCR product (Figure 3.11).

The human CMV promoter driving transgene expression in these studies is non-tissue specific. Therefore, Western blot analysis with the anti-c-myc antibody showed expression of the MC13-c-myc or Muta-1-c-myc cloned

subunits in several tissues from the PCR positive second generation pups (only brain and spinal cord are shown in Figure 3.12). The mature MC13-c-myc was detected in wild

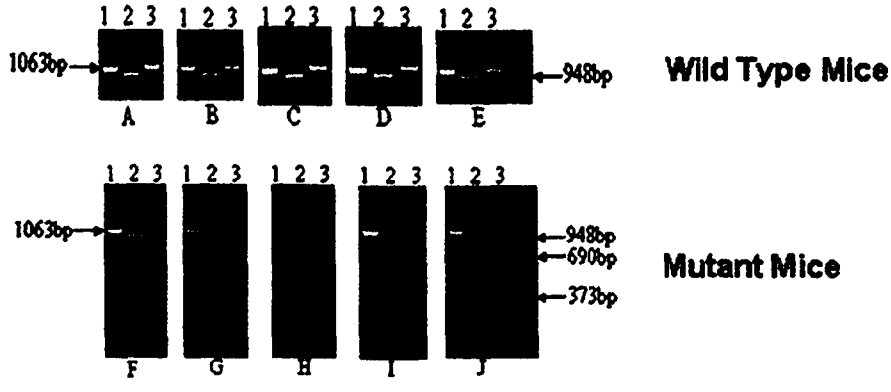


**Figure 3.11 - Restriction analysis of PCR products from positive transgenic mice.** Lanes 1: PCR products without digestion. The ~1.0kb bands remained intact; Lanes 2: PCR products digested with BamHI. PCR products from both the wild type and mutant mice contain a restriction site for BamHI. Digestion with this enzyme revealed two bands in each mouse: a 948bp band and a 115bp band (not shown); Lanes 3: PCR products digested with SfoI. SfoI digestion of PCR products from mutant mice yielded two bands: a 690bp band and a 373bp band while SfoI digestion of PCR products from wild type pups produced a 1063bp band, corresponding to the uncut PCR product.

type transgenic mice (W2) as a 24kDa band (Figure 3.12). The misprocessed cloned Muta-1-c-myc subunit was identified in mutant transgenic mice (M1 and M2) as a 26kDa band (Figure 3.12). As previously demonstrated in our mouse HT4 neuronal cell studies, these bands correspond to the respective processed mouse β5 subunits with a 2.1kDa c-myc

extension at the N-terminus. No precursor forms of MC13-c-myc and Muta-1-c-myc subunits were identified in the four mice tested. As previously discussed, this finding attests to the incorporation of the cloned subunits into the 20S proteasome particles.

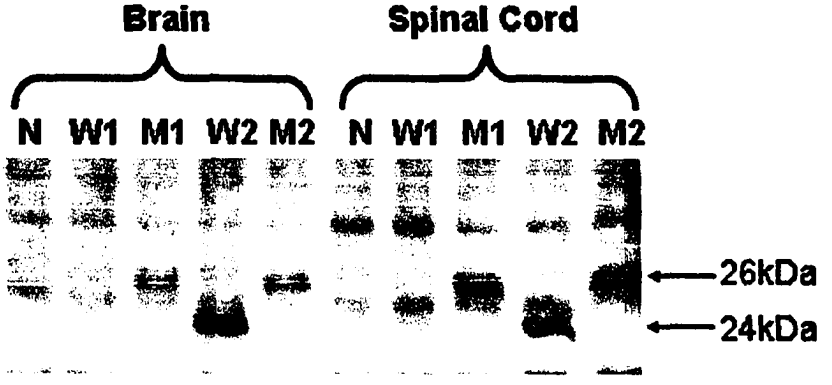


**Figure 3.12 - Expression of MC13-c-myc and Muta-1-c-myc in the CNS of transgenic mice.** Tissue samples from the brain and spinal cord of each PCR positive pup were homogenized in a 8.0M urea buffer. 50μg of protein from each sample were run on SDS-PAGE (12% gels). Western blots were probed with the anti-c-myc antibody. "N"- sample from a pup with a negative PCR result as a negative control; "W1" and "W2"- two positive MC13-c-myc transgenic pups; "M1" and "M2"- two positive Muta-1-c-myc transgenic pups.

The wild type mouse "W1" showed a positive PCR result; however, there was no MC13-c-myc protein detection in its CNS (Figure 3.12). This could be due to the so-called "position effect", in which the transgene is randomly incorporated into a chromosome region that is not active in

the CNS. Since these transgenic mice were established to develop a living model of neurodegeneration, we focused our studies on mice that expressed the cloned subunits in the brain and spinal cord.

The transgenic mice expressing the cloned subunits in the brain and spinal cord represent clinically relevant models for neurodegenerative pathogenesis associated with impairment of proteasome activity. Future studies with these transgenic mice will most likely provide insights into the underlying pathophysiological mechanisms of neurodegeneration.

# *Chapter IV*

# Discussion

A wide variety of neurodegenerative disorders are associated with the accumulation of ubiquitinated proteins in neuronal inclusions (Lowe et al., 2001). The inability of some neurons to degrade ubiquitinated proteins may result from a functional failure of the ubiquitin/proteasome pathway or from structural changes in the protein substrates rendering them inaccessible to the degradation component (Figueiredo-Pereira ME and Rockwell, 2001). Disruption of the ubiquitin/proteasome pathway can result from damaging events, such as oxidative stress (Shringarpure and Davies, 2002) and production of neurotoxic molecules, from mutations or from an aging-induced decrease in proteasome function (Carrard et al., 2002).

Most neurodegenerative disorders are age-dependent, long-term progressive diseases. Currently, there is no effective means of investigating the effects of a chronic loss of proteasome function in mammalian cells. In many studies, researchers investigate the role of proteasome dysfunction in neurodegeneration with proteasome inhibitors, but such agents are toxic, unstable, unsuitable for long-term studies and often unspecific. Our genetic approach to a decrease in proteasome activity overcomes

these difficulties thus providing a means to dissect the cellular responses to long-term proteasome impairment. We genetically manipulated the 20S proteasome activity in mouse neuronal HT4 cells by introducing a mutation in the active site of its MC13 subunit. This mouse β5 subunit accounts for the chymotrypsin-like activity of the 20S proteasome and carries out the rate-limiting step during protein degradation through the ubiquitin/proteasome pathway. Since studies have demonstrated that a functional β5 subunit is essential for cell survival, we expressed the mutant β5 subunit (Muta-1) in HT4 cells without interfering with the expression of endogenous wild type MC13 subunits. As our data indicate, impairment of proteasome activity due to expression of Muta-1 in this cellular system, is not dominant lethal under homeostatic conditions. However, it hypersensitizes the cells to oxidative stress resulting in the accumulation of ubiquitinated proteins in aggregates and leading to cell death. These findings clearly establish that selective proteasome dysfunction causes neuronal changes that are common to a broad range of human neurodegenerative disorders. Our cellular model consisting of mouse neuronal HT4 cells stably expressing Muta-1-c-myc is a useful tool to study the long-term effects of a

moderate decline in 20S proteasome activity alone or in combination with other stressors and their contribution to neurodegeneration. A better understanding of neuronal responses to these harmful conditions and their relationship to neuronal survival will facilitate the development of preventive approaches or treatments for neurodegeneration.

In addition to providing a model to study cellular responses to proteasome dysfunction, the Muta-1-c-myc stable transfectants provide a means to study inclusion body biogenesis. Accordingly, large aggregates containing ubiquitin-protein conjugates were detected in HT4 cells stably expressing Muta-1-c-myc. Some of the largest ubiquitin-protein aggregates caused nuclear distortions, similar to those detected in Lewy bodies in the substantia nigra of PD brains. Most of the vector and MC13-c-myc stable transfectants treated with cadmium exhibited only small ubiquitin-protein aggregates. The mechanisms leading to formation of such abnormal aggregates remain unclear and their role in the progression of the disease has yet to be elucidated (Tran and Miller, 1999). The fact that many components of the ubiquitin/proteasome pathway, such as ubiquitin C-terminal hydrolases and 26S proteasome

subunits, are found together with ubiquitin conjugates within inclusions in many neurodegenerative disorders (Lowe et al., 1990; Chai et al., 1999), strongly supports a role for this pathway in inclusion body biogenesis. It is possible that inclusions arise from a cellular attempt to compartmentalize accumulated proteins and prevent their interference with normal cell function. Their presence may also confer cytotoxic effects that can contribute to cellular damage associated with neurodegeneration. Aggregate size may be a pivotal determinant in their toxicity (Sharma et al., 1999). Small aggregates, as those found in the vector and MC13-c-myc stable transfectants treated with cadmium, did not lead to apparent cytotoxicity. Larger aggregates, as those detected in Muta-1-c-myc stable transfectants, may confer fatal effects by burdening the cell as the cytosolic or nuclear space is ultimately filled by the abnormal aggregates. The stable transfectants expressing Muta-1-c-myc, thus provide an excellent model to address the relationship between proteasome dysfunction, aggregate formation and neurodegeneration.

A wide variety of neurodegenerative disorders occur in the mature and fully developed CNS of adult individuals.

There is, therefore, a significant advantage in establishing an animal model of neurodegeneration expressing Muta-1-c-myc. Based on our cellular studies, we generated transgenic mice expressing Muta-1-c-myc, to examine whether the resulting decline in proteasome function contributes to CNS neurodegeneration. Our working hypothesis is that changes in proteasome activity due to expression of Muta-1-c-myc will alter protein removal in these mice, making them more susceptible to formation of protein aggregates, especially during aging or after stress conditions. Further studies on these transgenic mice will lead to a better understanding of the mechanisms underlying neurodegeneration associated with proteasome dysfunction and ultimately to the design of useful therapeutic alternatives.

As proteasome impairment seems to play a role in neurodegeneration, identification of mechanisms that may overcome the defect in proteasome activity could be of therapeutic significance. Pharmacological interventions designed to stimulate proteasome activity within the CNS may provide some therapeutic benefit. Such treatments could possibly be utilized to counteract the natural loss of proteasome activity that is observed to occur within the

CNS during normal aging, thus preventing or delaying age-related accumulation of, for example, oxidized proteins (Ding and Keller, 2001). Recent studies have identified a number of pharmacological proteasome activators, such as cardiolipin, which may ultimately provide the basis for such treatments in the future (Ruiz, I et al., 1993; Wilk and Chen, 1997; Wilk et al., 1999).

Another approach to the prevention of neurodegeneration associated with the accumulation of ubiquitinated proteins involves attenuating their aggregation tendency by over expressing molecular chaperones. This approach was successfully used to suppress disease progression in *Drosophila* models of PD expressing human α-synuclein (Auluck et al., 2002) or polyglutamine disorders expressing ataxin 3 (Chan et al., 2000). One of the molecular chaperones that is highly expressed in the brain is HSP110 (Hylander et al., 2000). Although HSP110 is known to protect cells and proteins from thermal damage, its potential for preventing protein aggregation in mammalian cells remains to be explored.

Finally, it may be possible in the future to increase the expression of specific proteasome subunits. Recent

studies identified a novel yeast protein known as RPN4 that is responsible for transcription regulation of a number of proteasome subunits (Xie and Varshavsky, 2001). Although no mammalian homologue was yet identified, these data raise the possibility of utilizing similar strategies to beneficially elevate proteasome expression in the CNS.

In conclusion, proteasome dysfunction might be a common link among the different environmental and genetic factors that are implicated in triggering a variety of neurodegenerative disorders. Cells must rely on the proteasome to remove mutant proteins or abnormal proteins produced under stress conditions. Impairment of proteasome function coupled to the selective vulnerability of specific subgroups of neuronal populations to different types of stress may thus be central to the development of familial as well as sporadic cases of neurodegeneration.

# *Chapter V*

# Appendix

# Sequencing of the *MC13—c-myc* in pcDNA3.1/hygro(-) with the $T_7$ (forward) Primer

```
  1  AGACCCAAGC  TGGCTAGCGT  TTAAACGGGC  CCTCTAGACT  CGAGCGGCCG
 51  CCACTGTGCT  GGATATCTGC  AGAATTCCAC  CACACTGGAC  TAGTGGATCC
101  CCCGGGCTGC  AGGAATTCGG  CACGAGGCCA  AGTGGTCATG  GCGTTACTGG
                                        137
151  ATCTGTGCGG  TGCCGCTCGG  GGACAGCGGC  CCGAGTGGGC  TGCCCTGGAT
201  GCGGGAAGCG  GGGGTCGCTC  GGACCCGGGA  CACTACAGTT  TCTCCGCGCA
251  AGCTCCGGAG  CTCGCACTTC  CCCGGGGAAT  GCAGCCCACC  GCATTCCTGA
301  GGTCCTTTGG  TGGTGACCAG  GAAAGGAATG  TTCAAATTGA  GATGGCCCAC
351  GGCACAACCA  CACTCGCCTT  CAAGTTCCAG  CATGGCGTCA  TCGTGGCTGT
       353  357
401  GGACTCCAGG  GCCACTGCAG  GGAGTTACAT  TAGCTCCTTA  AGGATGAACA
451  AAGTGATCGA  GATTAACCCT  TACCTGCTTG  GCACCATGTC  TGGTTGTGCA
501  GCCGACTGCC  AGTACTGGGA  GAGGCTGTTG  GCCAAGGAGT  GCAGGTTGTA
551  TTATCTTCGG  AATGGGGAAC  GCATCTCCGT  GTCTGCAGCA  TCCAAGCTGC
601  TTTCCAACAT  GATGCTGCAG  TACCGGGGGA  TGGGCCTCTC  CATGGGCAGC
651  ATGATCTGTG  GCTGGGACAA  GAAGGGACCA  GGACTTTACT  ACGTAGATGA
701  CAATGGGACT  CGGCTCTCGG  GACAGATGTT  TTCCACTGGC  AGCGGGAACA
751  CCTATGCCTA  CGGGTGATGG  ACAGTGGTTA  CCGGCAGGAC  CTCAGTCCTG
801  AAGAGCCTAC  GACCTTGGCC  GCAGAGCTAT  TGCTATGCTA  CCCACAGAGA
851  CAACTATTCT  GGAGGAGTCG  TCACATGTCC  ACATGAAGAA  GACGGTGGGT
901  GAAAATGGAN  AAN
                   913
```

Note: This sequence shows the sense-strand of the *MC13-c-myc*, from 5′ to 3′. 1-137: plasmid backbone; 138-353: prosequence of *MC13*; 354-356: the codon encoding the N-terminal threonine of mature MC13-c-myc; 357-913: partial *MC13*.

# Sequencing of the *MC13—c-myc* in pcDNA3.1/hygro(-) with the BGH (reverse) Primer

```
  1  AGCGGTTTAA  ACTTAAGCTT  GGTACCTACA  GATCCTCTTC  AGAGATGAGT
                                 25
 51  TTCTGCTCGA  GAGCGGCCTC  TCCGTACTTG  TACAGCAGGT  CACTGACATC
                 61
101  GGAACTCTCC  ACTTTCACCC  AACCGTCTTC  CTTCATGTGG  TACATGTTGA
151  CGACTCCTCC  AGAATAGTTG  TCTCTGTGGG  TAGCATAAGC  AATAGCTCTG
201  CGGCCAAGGT  CGTAGGCCTC  TTCAGGACTG  AGGTCCTGCC  GGTAACCACT
251  GTCCATCACC  CCGTAGGCAT  AGGTGTTCCC  GCTGCCAGTG  GAAAACATCT
301  GTCCCGAGAG  CCGAGTCCCA  TTGTCATCTA  CGTAGTAAAG  TCCTGGTCCC
351  TTCTTGTCCC  AGCCACAGAT  CATGCTGCCC  ATGGAGAGGC  CCATCCCCCG
401  GTACTGCAGC  ATCATGTTGG  AAAGCAGCTT  GGATGCTGCA  GACACGGAGA
451  TGCGTTCCCC  ATTCCGAAGA  TAATACAACC  TGCACTCCTT  GGCCAACAGC
501  CTCTCCCAGT  ACTGGCAGTC  GGCTGCACAA  CCAGACATGG  TGCCAAGCAG
551  GTAAGGGTTA  ATCTCGATCA  CTTTGTTCAT  CCTTAAGGAG  CTAATGTAAC
601  TCCCTGCAGT  GGCCCTGGAG  TCCACAGCCA  CGATGACGCC  ATGCTGGAAC
651  TTGAAGGCGA  GTGTGGTTGT  GCCGTGGGCC  ATCTCAATTT  GAACATTCCT
                        667     671
701  TTCCTGGTCA  CCACCAAAGG  ACCTCAGGAA  TGCGGTGGGC  TGCATTCCCC
751  GGGGAAGTGC  GAGCTCCGAG  CTTGCGCGGA  GAAACTGTAT  GTTCCCGGTC
801  CGAGCGACCC  CCGCTTTCCG  CATTCAGGGC  AGCCCACTCG  GGCCGTGTCC
851  CGAGCGGAC
               859
```

**Note: This sequence shows the antisense-strand of the *MC13-c-myc*, from 5′ to 3′. 1-25: plasmid backbone; 26-61: *c-myc* tag; 62-667: partial *MC13*; 668-670: the anti-codon for the N-terminal threonine of mature MC13-c-myc; 671-859: prosequence of *MC13*.**

# Sequencing of the *Muta-1–c-myc* in pcDNA3.1/hygro(-) with the $T_7$ (forward) Primer

```
  1  AGACCCAAGC  TGGCTAGCGT  TTAAACGGGC  CCTCTAGACT  CGAGCGGCCG
 51  CCACTGTGCT  GGATATCTGC  AGAATTCCAC  CACACTGGAC  TAGTGGATCC
101  CCCGGGCTGC  AGGAATTCGG  CACGAGGCCA  AGTGGTCATG  GCGTTACTGG
                                        137
151  ATCTGTGCGG  TGCCGCTCGG  GGACAGCGGC  CCGAGTGGGC  TGCCCTGGAT
201  GCGGGAAGCG  GGGGTCGCTC  GGACCCGGGA  CACTACAGTT  TCTCCGCGCA
251  AGCTCCGGAG  CTCGCACTTC  CCCGGGGAAT  GCAGCCCACC  GCATTCCTGA
301  GGTCCTTTGG  TGGTGACCAG  GAAAGGAATG  TTCAAATTGA  GATGGCCCAC
351  GGCGCCACCA  CACTCGCCTT  CAAGTTCCAG  CATGGCGTCA  TCGTGGCTGT
       353  357
401  GGACTCCAGG  GCCACTGCAG  GGAGTTACAT  TAGCTCCTTA  AGGATGAACA
451  AAGTGATCGA  GATTAACCCT  TACCTGCTTG  GCACCATGTC  TGGTTGTGCA
501  GCCGACTGCC  AGTACTGGGA  GAGGCTGTTG  GCCAAGGAGT  GCAGGTTGTA
551  TTATCTTCGG  AATGGGGAAC  GCATCTCCGT  GTCTGCAGCA  TCCAAGCTGC
601  TTTCCAACAT  GATGCTGCAG  TACCGGGGGA  TGGGCCTCTC  CATGGGCAGC
651  ATGATCTGTG  GCTGGGACAA  GAAGGGACCA  GGACTTTACT  ACGTAGATGA
701  CAATGGGACT  CGGCTCTCGG  GACAGATGTT  TTCCACTGGC  AGCGGGAACA
751  CCTATGCCTA  CGGGTGATGG  ACAGTGGTTA  CCGGCAGGAC  CTCAGTCCTG
801  AAGAGCCTAC  GACCTTGGCC  GCAGAGCTAT  TGCTATGCTA  CCCACAGAGA
851  CAACTATTCT  GGAGGAGTCG  TCACATGTCC  ACATGAAGAA  GACGGTGGGT
901  GAAAATGGAN  AAN
                   913
```

Note: This sequence shows the sense-strand of the *Muta-1-c-myc*, from 5′ to 3′. 1-137: plasmid backbone; 138-353: prosequence of *Muta-1*; 354-356: the codon encoding the N-terminal alanine of Muta-1; 357-913: partial *Muta-1*.

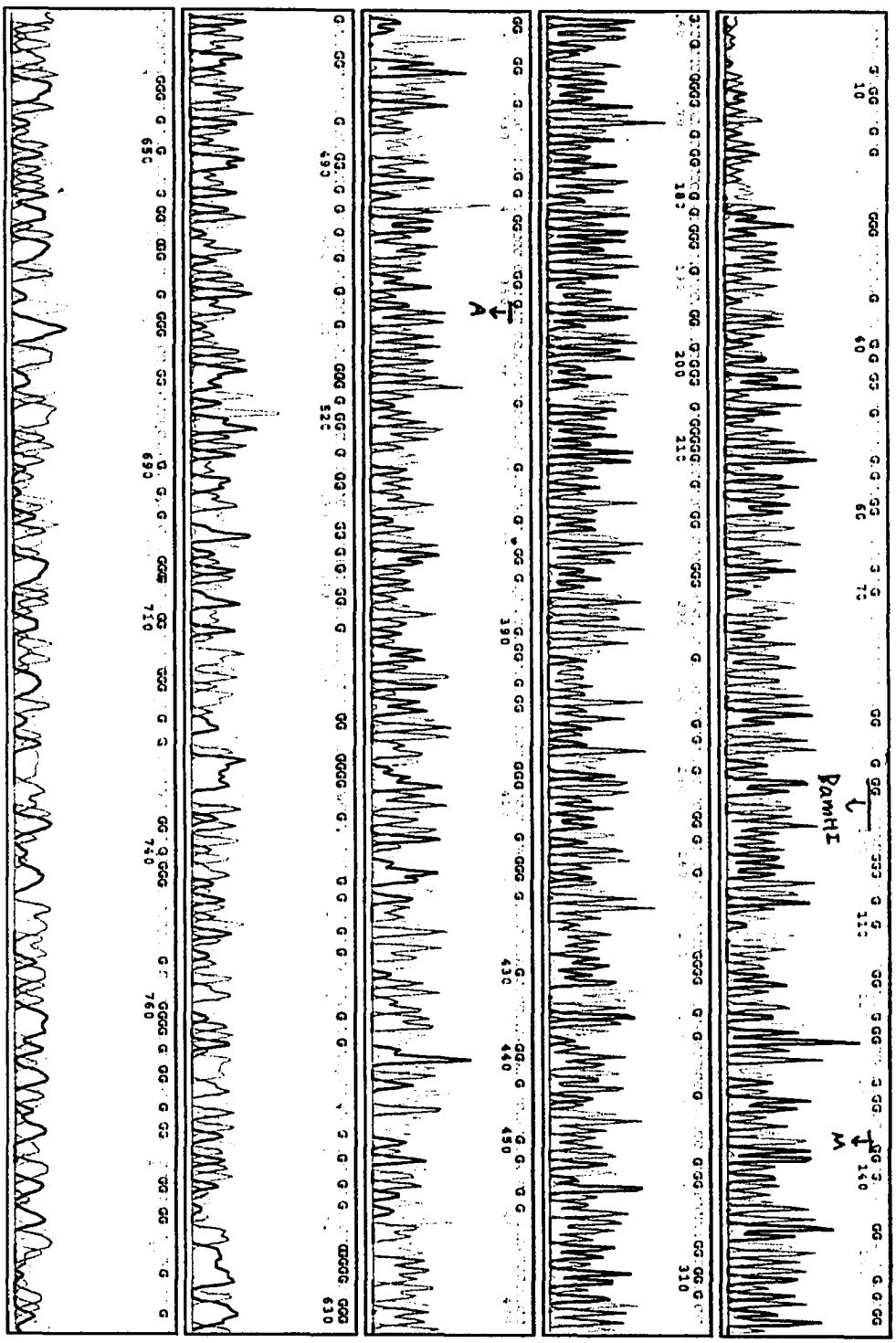

# Sequencing of the *Muta-1—c-myc* in pcDNA3.1/hygro(-) with the BGH (reverse) Primer

```
  1  AGCGGTTTAA  ACTTAAGCTT  GGTACCTACA  GATCCTCTTC  AGAGATGAGT
                                  25
 51  TTCTGCTCGA  GAGCGGCCTC  TCCGTACTTG  TACAGCAGGT  CACTGACATC
                 61
101  GGAACTCTCC  ACTTTCACCC  AACCGTCTTC  CTTCATGTGG  TACATGTTGA
151  CGACTCCTCC  AGAATAGTTG  TCTCTGTGGG  TAGCATAAGC  AATAGCTCTG
201  CGGCCAAGGT  CGTAGGCCTC  TTCAGGACTG  AGGTCCTGCC  GGTAACCACT
251  GTCCATCACC  CCGTAGGCAT  AGGTGTTCCC  GCTGCCAGTG  GAAAACATCT
301  GTCCCGAGAG  CCGAGTCCCA  TTGTCATCTA  CGTAGTAAAG  TCCTGGTCCC
351  TTCTTGTCCC  AGCCACAGAT  CATGCTGCCC  ATGGAGAGGC  CCATCCCCCG
401  GTACTGCAGC  ATCATGTTGG  AAAGCAGCTT  GGATGCTGCA  GACACGGAGA
451  TGCGTTCCCC  ATTCCGAAGA  TAATACAACC  TGCACTCCTT  GGCCAACAGC
501  CTCTCCCAGT  ACTGGCAGTC  GGCTGCACAA  CCAGACATGG  TGCCAAGCAG
551  GTAAGGGTTA  ATCTCGATCA  CTTTGTTCAT  CCTTAAGGAG  CTAATGTAAC
601  TCCCTGCAGT  GGCCCTGGAG  TCCACAGCCA  CGATGACGCC  ATGCTGGAAC
651  TTGAAGGCGA  GTGTGGTGGC  GCCGTGGGCC  ATCTCAATTT  GAACATTCCT
                        667   671
701  TTCCTGGTCA  CCACCAAAGG  ACCTCAGGAA  TGCGGTGGGC  TGCATTCCCC
751  GGGGAAGTGC  GAGCTCCGAG  CTTGCGCGGA  GAAACTGTAT  GTTCCCGGTC
801  CGAGCGACCC  CCGCTTTCCG  CATTCAGGGC  AGCCCACTCG  GGCCGTGTCC
851  CGAGCGGAC
                859
```

**Note: This sequence shows the antisense-strand of the *Muta-1-c-myc*, from 5′ to 3′. 1-25: plasmid backbone; 26-61: *c-myc* tag; 62-667: partial *Muta-1*; 668-670: the anti-codon for the N-terminal alanine of the *Muta-1*; 671-859: prosequence of *Muta-1*.**

# *Chapter VI*

# Reference List

1. Acan NL, Tezcan EF (1995) Inhibition kinetics of sheep brain glutathione reductase by cadmium ion. Biochem Mol Med 54: 33-37.

2. Aksenov MY, Aksenova MV, Markesbery WR, Butterfield DA (1998) Amyloid beta-peptide (1-40)-mediated oxidative stress in cultured hippocampal neurons. Protein carbonyl formation, CK BB expression, and the level of Cu, Zn, and Mn SOD mRNA. J Mol Neurosci 10: 181-192.

3. Albers DS, Augood SJ (2001) New insights into progressive supranuclear palsy. Trends Neurosci 24: 347-353.

4. Auluck PK, Chan HY, Trojanowski JQ, Lee VM, Bonini NM (2002) Chaperone suppression of alpha-synuclein toxicity in a Drosophila model for Parkinson's disease. Science 295: 865-868.

5. Beckman KB, Ames BN (1998) The free radical theory of aging matures. Physiol Rev 78: 547-581.

6. Belote JM, Fortier E (2002) Targeted expression of dominant negative proteasome mutants in Drosophila melanogaster. Genesis 34: 80-82.

7. Berlett BS, Stadtman ER (1997) Protein oxidation in aging, disease, and oxidative stress. J Biol Chem 272: 20313-20316.

8. Beyersmann D, Hechtenberg S (1997) Cadmium, gene regulation, and cellular signalling in mammalian cells. Toxicol Appl Pharmacol 144: 247-261.

9. Beyette JR, Hubbell T, Monaco JJ (2001) Purification of 20S proteasomes. Methods Mol Biol 156: 1-16.

10. Brannigan JA, Dodson G, Duggleby HJ, Moody PC, Smith JL, Tomchick DR, Murzin AG (1995) A protein catalytic framework with an N-terminal nucleophile is capable of self-activation. Nature 378: 416-419.

11. Bulteau AL, Petropoulos I, Friguet B (2000) Age-related alterations of proteasome structure and function in aging epidermis. Exp Gerontol. 35: 767-777.

12. Butterfield DA, Kanski J (2001) Brain protein oxidation in age-related neurodegenerative disorders that are associated with aggregated proteins. Mech Ageing Dev 122: 945-962.

13. Carrard G, Bulteau A, Petropoulos I, Friguet B (2002) Impairment of proteasome structure and function in aging. Int J Biochem Cell Biol 34: 1461.

14. Chai Y, Koppenhafer SL, Shoesmith SJ, Perez MK, Paulson HL (1999) Evidence for proteasome involvement in polyglutamine disease: localization to nuclear inclusions in SCA3/MJD and suppression of polyglutamine aggregation in vitro. Hum Mol Genet 8: 673-682.

15. Chan HY, Warrick JM, Gray-Board, Paulson HL, Bonini NM (2000) Mechanisms of chaperone suppression of polyglutamine disease: selectivity, synergy and modulation of protein solubility in Drosophila. Hum Mol Genet 9: 2811-2820.

16. Chao CC, Ma YS, Stadtman ER (1997) Modification of protein surface hydrophobicity and methionine oxidation by oxidative systems. Proc Natl Acad Sci U S A 94: 2969-2974.

17. Chen P, Hochstrasser M (1996) Autocatalytic subunit processing couples active site formation in the 20S proteasome to completion of assembly. Cell 86: 961-972.

18. Chun HS, Gibson GE, DeGiorgio LA, Zhang H, Kidd VJ, Son JH (2001) Dopaminergic cell death induced by MPP(+), oxidant and specific neurotoxicants shares the common molecular mechanism. J Neurochem 76: 1010-1021.

19. Chung CH, Baek SH (1999) Deubiquitinating enzymes: their diversity and emerging roles. Biochem Biophys Res Commun 266: 633-640.

20. Conconi M, Friguet B (1997) Proteasome inactivation upon aging and on oxidation-effect of HSP 90. Mol Biol Rep 24: 45-50.

21. Cook WJ, Jeffrey LC, Kasperek E, Pickart CM (1994) Structure of tetraubiquitin shows how multiubiquitin chains can be formed. J Mol Biol 236: 601-609.

22. Coux O, Tanaka K, Goldberg AL (1996) Structure and functions of the 20S and 26S proteasomes. Annu Rev Biochem 65: 801-847.

23. Davies KJ (1987) Protein damage and degradation by oxygen radicals. I. general aspects. J Biol Chem 262: 9895-9901.

24. DeMartino GN, Slaughter CA (1999a) The proteasome, a novel protease regulated by multiple mechanisms. J Biol Chem 274: 22123-22126.

25. DeMartino GN, Slaughter CA (1999b) The proteasome, a novel protease regulated by multiple mechanisms. J Biol Chem 274: 22123-22126.

26. Dick TP, Nussbaum AK, Deeg M, Heinemeyer W, Groll M, Schirle M, Keilholz W, Stevanovic S, Wolf DH, Huber R, Rammensee HG, Schild H (1998) Contribution of proteasomal beta-subunits to the cleavage of peptide substrates analyzed with yeast mutants. J Biol Chem 273: 25637-25646.

27. Ding Q, Keller JN (2001) Proteasomes and proteasome inhibition in the central nervous system. Free Radic Biol Med 31: 574-584.

28. Fahn S, Cohen G (1992) The oxidant stress hypothesis in Parkinson's disease: evidence supporting it. Ann Neurol 32: 804-812.

29. Figueiredo-Pereira ME, Rockwell P (2001) The ubiquitin/proteasome pathway in neurological disorders. In: Proteolysis in the pathophysiology of neurodegenerative disease (Banik NL, Lajtha A, Smith M, eds), New York, N.Y.: Kluwer Academic/Plenum Publishers.

30. Figueiredo-Pereira ME, Cohen G (1999) The ubiquitin/proteasome pathway: friend or foe in zinc-, cadmium-, and H2O2-induced neuronal oxidative stress. Mol Biol Rep 26: 65-69.

31. Figueiredo-Pereira ME, Yakushin S, Cohen G (1998) Disruption of the intracellular sulfhydryl homeostasis by cadmium- induced oxidative stress leads to protein thiolation and ubiquitination in neuronal cells. J Biol Chem 273: 12703-12709.

32. Frentzel S, Graf U, Hammerling GJ, Kloetzel PM (1992) Isolation and characterization of the MHC linked beta-type proteasome subunit MC13 cDNA. FEBS Lett 302: 121-125.

33. Friguet B, Szweda LI (1997) Inhibition of the multicatalytic proteinase (proteasome) by 4-hydroxy-2- nonenal cross-linked protein. FEBS Lett 405: 21-25.

34. Giasson BI, Ischiropoulos H, Lee VM, Trojanowski JQ (2002) The relationship between oxidative/nitrative stress and pathological inclusions in Alzheimer's and Parkinson's diseases. Free Radic Biol Med 32: 1264-1275.

35. Glickman MH, Ciechanover A (2002) The ubiquitin-proteasome proteolytic pathway: destruction for the sake of construction. Physiol Rev 82: 373-428.

36. Goldberg AL, Rock K (2002) Not just research tools--proteasome inhibitors offer therapeutic promise. Nat Med 8: 338-340.

37. Groll M, Ditzel L, Lowe J, Stock D, Bochtler M, Bartunik HD, Huber R (1997) Structure of 20S proteasome from yeast at 2.4 A resolution. Nature 386: 463-471.

38. Groll M, Heinemeyer W, Jager S, Ullrich T, Bochtler M, Wolf DH, Huber R (1999) The catalytic sites of 20S proteasomes and their role in subunit maturation: a mutational and crystallographic study. Proc Natl Acad Sci U S A 96: 10976-10983.

39. Grune T, Reinheckel T, Davies KJ (1997) Degradation of oxidized proteins in mammalian cells. FASEB J 11: 526-534.

40. Hechtenberg S, Beyersmann D (1994) Interference of cadmium with ATP-stimulated nuclear calcium uptake. Environ Health Perspect 102 Suppl 3: 265-267.

41. Heinemeyer W, Gruhler A, Mohrle V, Mahe Y, Wolf DH (1993) PRE2, highly homologous to the human major histocompatibility complex- linked RING10 gene, codes for a yeast proteasome subunit necessary for chrymotryptic activity and degradation of ubiquitinated proteins. J Biol Chem 268: 5115-5120.

42. Heinemeyer W, Kleinschmidt JA, Saidowsky J, Escher C, Wolf DH (1991) Proteinase yscE, the yeast proteasome/multicatalytic-multifunctional proteinase: mutants unravel its function in stress induced proteolysis and uncover its necessity for cell survival. EMBO J 10: 555-562.

43. Hinkle PM, Osborne ME (1994) Cadmium toxicity in rat pheochromocytoma cells: studies on the mechanism of uptake. Toxicol Appl Pharmacol 124: 91-98.

44. Hochstrasser M (1995) Ubiquitin, proteasomes, and the regulation of intracellular protein degradation. Curr Opin Cell Biol 7: 215-223.

45. Hylander BL, Chen X, Graf PC, Subjeck JR (2000) The distribution and localization of hsp110 in brain. Brain Res 869: 49-55.

46. Jenner P (2001) Parkinson's disease, pesticides and mitochondrial dysfunction. Trends Neurosci 24: 245-247.

47. Jungmann J, Reins HA, Schobert C, Jentsch S (1993) Resistance to cadmium mediated by ubiquitin-dependent proteolysis. Nature 361: 369-371.

48. Keller JN, Hanni KB, Markesbery WR (2000a) Impaired proteasome function in Alzheimer's disease. J Neurochem 75: 436-439.

49. Keller JN, Huang FF, Zhu H, Yu J, Ho YS, Kindy TS (2000b) Oxidative stress-associated impairment of proteasome activity during ischemia-reperfusion injury. J Cereb Blood Flow Metab 20: 1467-1473.

50. Kim JI, Choi SI, Kim NH, Jin JK, Choi EK, Carp RI, Kim YS (2001) Oxidative stress and neurodegeneration in prion diseases. Ann N Y Acad Sci 928: 182-186.

51. Kisselev AF, Akopian TN, Castillo V, Goldberg AL (1999) Proteasome active sites allosterically regulate each other, suggesting a cyclical bite-chew mechanism for protein breakdown. Mol Cell 4: 395-402.

52. Kjellstrom T (1971) A mathematical model for the accumulation of cadmium in human kidney cortex. Nord Hyg Tidskr 52: 111-119.

53. Klein JA, Ackerman SL (2003) Oxidative stress, cell cycle, and neurodegeneration. J Clin Invest 111: 785-793.

54. Klug S, Planas-Bohne F, Taylor DM (1988) Factors influencing the uptake of cadmium into cells in vitro. Hum Toxicol 7: 545-549.

55. Koegl M, Hoppe T, Schlenker S, Ulrich HD, Mayer TU, Jentsch S (1999) A novel ubiquitination factor, E4, is involved in multiubiquitin chain assembly. Cell 96: 635-644.

56. Lee CK, Klopp RG, Weindruch R, Prolla TA (1999) Gene expression profile of aging and its retardation by caloric restriction. Science 285: 1390-1393.

57. Lowe J, Blanchard A, Morrell K, Lennox G, Reynolds L, Billett M, Landon M, Mayer RJ (1988) Ubiquitin is a common factor in intermediate filament inclusion bodies of diverse type in man, including those of Parkinson's disease, Pick's disease, and Alzheimer's disease, as well as Rosenthal fibres in cerebellar astrocytomas, cytoplasmic bodies in muscle, and mallory bodies in alcoholic liver disease. J Pathol 155: 9-15.

58. Lowe J, Mayer J, Landon M, Layfield R (2001) Ubiquitin and the molecular pathology of neurodegenerative diseases. Adv Exp Med Biol 487: 169-186.

59. Lowe J, McDermott H, Landon M, Mayer RJ, Wilkinson KD (1990) Ubiquitin carboxyl-terminal hydrolase (PGP 9.5) is selectively present in ubiquitinated inclusion bodies characteristic of human neurodegenerative diseases. J Pathol 161: 153-160.

60. Ly DH, Lockhart DJ, Lerner RA, Schultz PG (2000) Mitotic misregulation and human aging. Science 287: 2486-2492.

61. Markesbery WR, Carney JM (1999) Oxidative alterations in Alzheimer's disease. Brain Pathol 9: 133-146.

62. Mayer RJ, Arnold J, Laszlo L, Landon M, Lowe J (1991) Ubiquitin in health and disease. Biochim Biophys Acta 1089: 141-157.

63. McNaught KS, Jenner P (2001) Proteasomal function is impaired in substantia nigra in Parkinson's disease. Neurosci Lett 297: 191-194.

64. Melov S, Schneider JA, Day BJ, Hinerfeld D, Coskun P, Mirra SS, Crapo JD, Wallace DC (1998) A novel neurological phenotype in mice lacking mitochondrial manganese superoxide dismutase. Nat Genet 18: 159-163.

65. Mosmann T (1983) Rapid colorimetric assay for cellular growth and survival: application to proliferation and cytotoxicity assays. J Immunol Methods 65: 55-63.

66. Nakagawara A, Nathan CF, Cohn ZA (1981) Hydrogen peroxide metabolism in human monocytes during differentiation in vitro. J Clin Invest 68: 1243-1252.

67. Okada K, Wangpoengtrakul C, Osawa T, Toyokuni S, Tanaka K, Uchida K (1999) 4-Hydroxy-2-nonenal-mediated impairment of intracellular proteolysis during oxidative stress. Identification of proteasomes as target molecules. J Biol Chem 274: 23787-23793.

68. Pickart CM (1997) Targeting of substrates to the 26S proteasome. FASEB J 11: 1055-1066.

69. Pihl RO, Parkes M (1977) Hair element content in learning disabled children. Science 198: 204-206.

70. Ramos PC, Hockendorff J, Johnson ES, Varshavsky A, Dohmen RJ (1998) Ump1p is required for proper maturation of the 20S proteasome and becomes its substrate upon completion of the assembly. Cell 92: 489-499.

71. Rockwell P, Yuan HM, Magnusson R, Figueiredo-Pereira ME (2000) Proteasome inhibition in neuronal cells induces a proinflammatory response manifested by upregulation of cyclooxygenase-2, its accumulation as ubiquitin conjugates, and production of the prostaglandin PGE2. Arch Biochem Biophys 374.

72. Ruiz dM, I, Mahillo E, Arribas J, Castano JG (1993) Kinetic mechanism of activation by cardiolipin (diphosphatidylglycerol) of the rat liver multicatalytic proteinase. Biochem J 296 ( Pt 1): 93-97.

73. Sadis S, Atienza CJ, Finley D (1995) Synthetic signals for ubiquitin-dependent proteolysis. Mol Cell Biol 15: 4086-4094.

74. Scherrer K, Bey F (1994) The prosomes (multicatalytic proteinases; proteasomes) and their relationship to the untranslated messenger ribonucleoproteins, the cytoskeleton, and cell differentiation. Prog Nucleic Acid Res Mol Biol 49: 1-64.

75. Schmidt M, Kloetzel PM (1997) Biogenesis of eukaryotic 20S proteasomes: the complex maturation pathway of a complex enzyme. FASEB J 11: 1235-1243.

76. Schmidtke G, Kraft R, Kostka S, Henklein P, Frommel C, Lowe J, Huber R, Kloetzel PM, Schmidt M (1996) Analysis of mammalian 20S proteasome biogenesis: the maturation of beta- subunits is an ordered two-step mechanism involving autocatalysis. EMBO J 15: 6887-6898.

77. Schulz JB, Dichgans J (1999) Molecular pathogenesis of movement disorders: are protein aggregates a common link in neuronal degeneration? Curr Opin Neurol 12: 433-439.

78. Shang F, Nowell TR, Jr., Taylor A (2001) Removal of oxidatively damaged proteins from lens cells by the ubiquitin-proteasome pathway. Exp Eye Res 73: 229-238.

79. Shang F, Taylor A (1995) Oxidative stress and recovery from oxidative stress are associated with altered ubiquitin conjugating and proteolytic activities in bovine lens epithelial cells. Biochem J 307 ( Pt 1): 297-303.

80. Sharma D, Sharma S, Pasha S, Brahmachari SK (1999) Peptide models for inherited neurodegenerative disorders: conformation and aggregation properties of long polyglutamine peptides with and without interruptions. FEBS Lett 456: 181-185.

81. Shringarpure R, Davies KJ (2002) Protein turnover by the proteasome in aging and disease(1,2). Free Radic Biol Med 32: 1084-1089.

82. Shringarpure R, Grune T, Mehlhase J, Davies KJ (2003) Ubiquitin conjugation is not required for the degradation of oxidized proteins by proteasome. J Biol Chem 278: 311-318.

83. Shukla GS, Chandra SV (1987) Concurrent exposure to lead, manganese, and cadmium and their distribution to various brain regions, liver, kidney, and testis of growing rats. Arch Environ Contam Toxicol 16: 303-310.

84. Stohs SJ, Bagchi D (1995) Oxidative mechanisms in the toxicity of metal ions. Free Radic Biol Med 18: 321-336.

85. Tanaka K, Ichihara A (1989) Half-life of proteasomes (multiprotease complexes) in rat liver. Biochem Biophys Res Commun 159: 1309-1315.

86. Tran PB, Miller RJ (1999) Aggregates in neurodegenerative disease: crowds and power? Trends Neurosci 22: 194-197.

87. Tsuchiya K, Sugita M, Seki Y (1976) Mathematical derivation of the biological half-time of cadmium in human organs based on the accumulation of the metal in the organs. Keio J Med 25: 73-82.

88. Van Remmen H, Williams MD, Heydari AR, Takahashi R, Chung HY, Yu BP, Richardson A (1996) Expression of genes coding for antioxidant enzymes and heat shock proteins is altered in primary cultures of rat hepatocytes. J Cell Physiol 166: 453-460.

89. Wang R, Chait BT, Wolf I, Kohanski RA, Cardozo C (1999) Lysozyme degradation by the bovine multicatalytic proteinase complex (Proteasome): evidence for a nonprocessive mode of degradation. Biochemistry 38: 14573-14581.

90. Whittemore SR, Holets VR, Keane RW, Levy DJ, McKay RD (1991) Transplantation of a temperature-sensitive, nerve growth factor- secreting, neuroblastoma cell line into adult rats with fimbria-fornix lesions rescues cholinergic septal neurons. J Neurosci Res 28: 156-170.

91. Wilk S, Chen WE (1997) Synthetic peptide-based activators of the proteasome. Mol Biol Rep 24: 119-124.

92. Wilk S, Chen WE, Magnusson RP (1999) Modulators of the activation of the proteasome by PA28 (11S reg). Mol Biol Rep 26: 39-44.

93. Wilk S, Orlowski M (1983) Evidence that pituitary cation-sensitive neutral endopeptidase is a multicatalytic protease complex. J Neurochem 40: 842-849.

94. Wilkinson KD (1997) Regulation of ubiquitin-dependent processes by deubiquitinating enzymes. FASEB J 11: 1245-1256.

95. Xie Y, Varshavsky A (2001) RPN4 is a ligand, substrate, and transcriptional regulator of the 26S proteasome: a negative feedback circuit. Proc Natl Acad Sci U S A 98: 3056-3061.

96. Yokota T, Igarashi K, Uchihara T, Jishage K, Tomita H, Inaba A, Li Y, Arita M, Suzuki H, Mizusawa H, Arai H (2001) Delayed-onset ataxia in mice lacking alpha -tocopherol transfer protein: model for neuronal degeneration caused by chronic oxidative stress. Proc Natl Acad Sci U S A 98: 15185-15190.